UNIVERSITY OF CALGARY

Photocatalytic Treatment of Wastewater: A Model for a Fast Process Monitoring Analysis Method

by

Kathleen Marie Ann Tremblay

A THESIS

SUBMITTED TO THE FACULTY OF GRADUATE STUDIES

IN PARTIAL FULFILMENT OF THE REQUIREMENTS FOR THE

DEGREE OF MASTER OF SCIENCE

DEPARTMENT OF CHEMISTRY

CALGARY, ALBERTA

September, 2001

National Library of Canada
Acquisitions and Bibliographic Services
395 Wellington Street
Ottawa ON K1A 0N4
Canada

Bibliothèque nationale du Canada
Acquisitions et services bibliographiques
395, rue Wellington
Ottawa ON K1A 0N4
Canada

Your file Votre référence

Our file Notre référence

0-612-65139-8

Canada

Abstract

Whitewater has four main classes of compounds of interest. These are fatty acids and resin acids, lignins, triglycerides, and sterol esters. A model compound is chosen for each class and will constitute a model for a fast and simple analysis of white water. The model is used for the analysis of a model water and real white water, the results for each compared.

Each model compound, model water, and real whitewater was treated by four different methods. The first being direct photolysis, the second being photolysis with UCPG204 catalyst, the third being photolysis with the catalyst and hydrogen peroxide, and fourth method being photolysis with degussa P25 TiO_2. These four methods were chosen to compare the photocatalytic activity of the catalyst, and study its efficiency. The experiments show treatment with degussa P25 TiO_2 to be the method of choice. Past experiments show that this is false; therefore the irradiation time chosen was somewhat inadequate.

The period of irradiation of 24 hours was chosen knowing that the probability of mineralization would be at a minimum. This time frame was chosen to monitor the degradation of each compound enabling construction of the model.

Acknowledgements

This work was made possible in part by funding from the Sustainable Forest Management of the Network Centers of Excellence.

I would like to thank Dr. Cooper H. Langford who took me into his group and put this project together for me. I would also like to thank him for his guidance and assistance.

I would like to thank Dr. E. A. Dixon for sitting on my supervisory committee and offering her advice. In addition to this I would like to thank Dr. Kevin Thurbide and Dr. Gopal Achari for sitting on my defence committee.

I would like to thank Dr. Aldo Bruccoleri, Tiona Todoruk, Dr. Robert Cook, and Lisa Knight for their many fruitful intellectual discussions. In addition to this I would like to thank Jeremy Wulff and Mike Hamilton for their help with the mechanisms.

I would like to thank Greta Prihodko and Bonnie King for making my time here a little more pleasant. I would also like to thank Mike Siewert, Kim Wagstaff, and Keith Collins for the many times they saved my life when computers and instruments just didn't work.

Many thanks go to Lisa Knight, Tiona Todoruk, Yanjun Chang, Preston Chase, Lee Henderson, Lisa Sneed, Melanie Roy, and the rest, you know who you are, for the fun-filled silly times and laughs.

To my family and friends

TABLE OF CONTENTS

Approval Page.....ii
Abstract.....iii
Acknowledgements.....iv
Dedication.....v
Table of Contents.....vi-vii
List of Figures.....viii-xi
List of Tables..... xi

1 Photocatalysis and Pulpmill Wastes.....1

1.1 Brief History of Photocatalysis.....1
1.2 Fundamentals of Titanium Dioxide Photocatalysis.....2
1.2.1 General Considerations.....2
1.2.2 Integrated Photocatalyst and Adsorbants.....4
1.3 Pulpmill Waste.....5
1.3.1 Brief History of Pulping.....5
1.3.2 Components of Waste Streams.....8
1.3.2.1 Different Classes of Components.....8
Cellulose.....8
Hemicellulose.....8-9
Lignin.....9-10
Extractives.....11

1.3.2.2 Components of Environmental Concern.....11
1.3.2.3 Regulatory Parameters for Discharge.....12
1.4 Past Observations on Photocatalytic Treatment of Pulpmill Streams ..16
1.5 Goals of Project.....19
1.5.1 Goal of Simplified Analysis.....19
1.5.2 Goal of Establishing Relative Efficiency of Different Component Oxidation.....21
References.....22

2 Experimental.....25

2.1 Materials.....25
2.2 Analytical procedures.....26
2.3 Photocatalytic Procedures.....27
2.3.1 Reactor Description.....27
2.3.2 Oxidation Procedures.....27
2.3.3 Light Intensity Measurements by Ferrioxalate Actinometry.....28
References.....32

3 Results.....33

3.1 Fatty Acids and Resin Acids.....34
3.2 Sterol Esters.....41
3.3 Triglycerides.....43
3.4 Lignins.....45

3.5 Model Whitewater.....53
3.6 Whitewater.....63
3.7 Comparison of Model Whitewater with Real Whitewater.....74

4 Discussion.....77

4.1 Hydrogen Peroxide Coupled with Catalytic Degradation.....77
4.2 Development of a New Method.....78
4.3 General Conclusions.....80
References.....81

Appendix 1.....82

List of Figures

Chapter 1

Figure 1.2.1-1. Irradiated TiO_2 particle.....3

Figure 1.3.1-1. Process of making the Egyptian style writing material.....6

Figure 1.3.1-2. Modern method of pulping, closed pulping where filtrate is recycled and reused.....7

Figure 1.3.2-1. Cellulose molecule.....8

Figure 1.3.2-2. structure of softwood lignin.....10

Figure 1.3.2-2. Source of extractives found in wood.....11

Figure 1.5-1. Present method for extraction of target compounds.....20

Chapter 3

Figure 3.1-1. HLPC chromatogram for vinyl acetic acid.....34

Figure 3.1-2. HPLC chromatogram for abietic acid.....37

Figure 3.1-3. HPLC chromatogram for abietic acid, initial 24 hour direct photolysis 38

Figure 3.2-1. HPLC chromatogram for the treatment on ethylnonanoate with the supported catalyst.....41

Figure 3.3-1. HPLC chromatogram for the treatment of triacetin with the supported catalyst.....43

Figure 3.4-1. HPLC chromatogram of lignin treated with the supported catalyst.....45

Figure 3.4-2. UV-visible spectra after direct photolysis on lignin alkali.....46

Figure 3.4-3. UV-visible spectra after lignin alkali treatment with supported catalyst 47

Figure 3.4-4. UV-visible spectra after lignin alkali treatment with catalyst and hydrogen peroxide.....47

Figure 3.4-5. UV-visible spectra of lignin alkali treatment with titanium dioxide.....48

Figure 3.4-6. Differential UV-visible spectra, showing changes occurring during direct photolysis.....49

Figure 3.4-7. Differential UV-visible spectra, showing changes occurring during photolysis with the catalyst.....50

Figure 3.4-8. Differential UV-visible spectra, showing changes occurring during photolysis with the catalyst and hydrogen peroxide.....50

Figure 3.4-9. Differential UV-visible spectra, showing changes occurring during photolysis with titanium dioxide.....51

Figure 3.5-1. HPLC chromatogram of aqueous extract of model water treatment with the supported catalyst.....54

Figure 3.5-2. a) and b) HPLC chromatogram of the organic extract of the model water treatment with the supported catalyst.....55

Figure 3.5-3. UV-visible spectra after direct photolysis on the aqueous extract of model water.....56

Figure 3.5-4. UV-visible spectra after treatment with the catalyst on the aqueous extract of model water.....57

Figure 3.5-5. UV-visible spectra after treatment with the catalyst and hydrogen peroxide on the aqueous extract of model water.....57

Figure 3.5-6. UV-visible spectra after treatment with titanium dioxide on the aqueous extract of model water.....58

Figure 3.5-7. Differential UV-visible spectra, showing changes occurring during direct photolysis.....58

Figure 3.5-8. Differential UV-visible spectra, showing changes occurring during photolysis with the supported catalyst 59

Figure 3.5-9. Differential UV-visible spectra, showing changes occurring during photolysis with the supported catalyst and hydrogen peroxide.....60

Figure 3.5-10. Differential UV-visible spectra, showing changes occurring during photolysis with titanium dioxide.....61

Figure 3.6-1. HPLC chromatogram of aqueous extract of real whitewater treatment with the supported catalyst.....64

Figure 3.6-2. a) and b) HPLC chromatogram of the organic extract of the real whitewater treatment with the supported catalyst.....65

Figure 3.6-3. UV-visible spectra after direct photolysis on the aqueous extract of real whitewater.....66

Figure 3.6-4. UV-visible spectra after treatment with the catalyst on the aqueous extract of the real whitewater.....67

Figure 3.6-5. UV-visible spectra after treatment with the catalyst and hydrogen peroxide on the aqueous extract of the real water.....68

Figure 3.6-6. UV-visible spectra after treatment with titanium dioxide on the aqueous extract after real whitewater.....68

Figure 3.6-7. Differential UV-visible spectra, showing changes occurring during direct photolysis.....69

Figure 3.6-8. Differential UV-visible spectra, showing changes occurring during photolysis with the supported catalyst 70

Figure 3.6-9. Differential UV-visible spectra, showing changes occurring during photolysis with the supported catalyst and hydrogen peroxide.....71

Figure 3.6-10. Differential UV-visible spectra, showing changes occurring during photolysis with titanium dioxide.....72

List of Tables

Table 1.3.3-1. Sample threshold odour numbers.....13

Table 1.3.3-2. Regulatory parameters for pulpmill waste emissions for the protection of fresh water aquatic life 15

Table 1.4-2. Previous results of treatments on wastewater.....17

Table 3.1-1. Summary of results of photocatalytic treatment of an aqueous vinyl acetic acid solution.....35

Table 3.1-2. Summary of results of photocatalytic treatment of an aqueous abietic acid solution.....39, 40

Table 3.2-1. Summary of results of photocatalytic treatment of an aqueous solution of ethylnonanote 42

Table 3.3-1. Summary of results of photocatalytic treatment of an aqueous triacetin solution.....44

Table 3.4-1. Summary of results of photocatalytic treatment of an aqueous solution of lignin alkali.....52

Table 3.5-1. Summary of results of degradation of model water.....62, 63

Table 3.6-1. Concentrations of compounds in model water throughout the 24 hour irradiation period.....73, 74

1 Photocatalysis and Pulpmill Wastes

1.1 Brief History of Photocatalysis

We are surrounded by photochemistry everyday, we see it in the green colour of grass and leaves every summer day. However, the first mention of photocatalysis was by Plotnikov in the 1930's in his book entitled Allgemeine Photochemie[28]. The next major development followed in the 1950's when Markham and Laidler performed a kinetic study of photo oxidation on the surface of zinc oxide in an aqueous suspension[28].

By the 1970's researchers started to perform surface studies on photocatalysts like Zinc Oxide and Titanium Dioxide[4],[10],[21],[22],[23],[24],[25],[26]. Titanium Dioxide may come in the anatase or the rutile form. Degussa P25 Titanium Dioxide contains both the anatase and rutile form[4],[25]. Curiously, this mixture long stood as the standard in photocatalysis with high reactivity. In the 1970's solar energy was being studied due to a need for more available renewable resources and environmental concerns; photochemistry was looked upon for the storage and usage of solar energy[8]. In 1972 Fujishima and Honda had a breakthrough for the photolysis of water with a semiconductor electrode, which could also be a solar powered cell[36]. The next big breakthrough in photochemistry occurred in 1976 when Carey and Oliver developed a method for measuring the variation in quantum efficiency with intensity[37] .The interest in using titania as a photocatalyst has since been revived in the 1990's[20].

In the 1980's and 1990's there came an increasing concern for environmental preservation and cleanup. As a result some environmental scientists have looked at photochemistry for air, water, and soil cleanup [13],[17],[19],[20],[27]. TiO_2 catalyzed photochemistry can accomplish the mineralization, which is the degradation of organic compounds to H_2O and CO_2 and its inorganic substituants if the organic compound should have any, of many different organic compounds[10],[19],[20].

1.2 Fundamentals of Titanium Dioxide Photocatalysis

1.2.1 General Considerations

It is known that photocatalysts can be either homogeneous or heterogeneous. In a system where a homogeneous photocatalyst is used, the photocatalytic reaction takes place in a homogeneous liquid phase. Examples of such photocatalysts include dyes[8],soluble metal catalysts like copper complexes[9], tin chloride[5], palladium chloride[5] Fenton's Reagent[13], and hydrogen peroxide[3],[17]. On the other hand, if a heterogeneous photocatalyst is used the photocatalyst and reactant are present in different phases and the photocatalytic reaction occurs at their interface. Examples of heterogeneous photocatalysts include polyoxometallates such as $Cs_3PW_{12}O_{40}$[11],[12], TiO_2 in the

colloidal[11] and powdered form[14],[15],[16],[18] or dyes supported on glass, sand and other materials[7].

Solid TiO_2 absorbs light in the near UV (~350 nm) causing an electron from the valence band to be excited across the band gap of +3.0 eV up to the conduction band containing free electrons. It has the ability to produce conductivity similar to that of metals. The carriers may be trapped at or near the TiO_2 particle surface; thus, enabling electron transfer reactions across the interface with a large variety of organic molecules absorbed on the TiO_2 surface from the solution. The potential of the trapped hole carrier is +3.2 V and the electron has a potential of 0 V on the hydrogen scale. This makes the hole a powerful oxidizing agent and the electron a good reducing agent. The hole can generate a hydroxyl radical at the surface or a one electron oxidation of a wide range of adsorbed organic molecules can be initiated (see Figure 1.2.1-1).

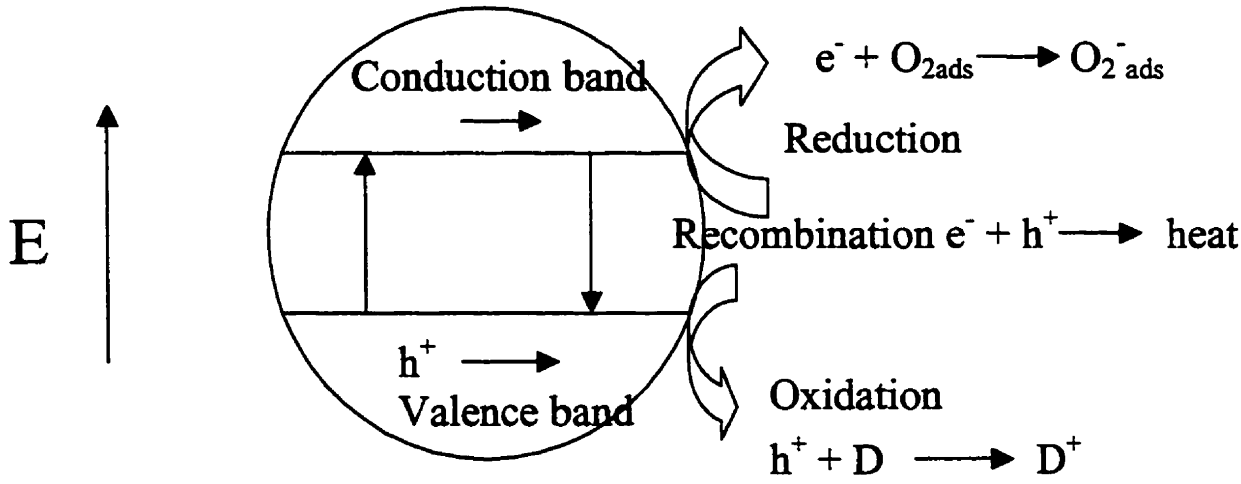

Figure 1.2.1-1: Irradiated TiO_2 particle

The electron is captured by O_2 to generate the reactive superoxide ion. For the above reasons the illuminated TiO_2 surface is an extremely attractive catalyst for the initiation of the oxidation of a wide range of organic compounds. In most cases the oxidation can proceed to mineralization where the final products are CO_2, H_2O, and inorganic ions of other elements that may be present in the organic molecule. As stated earlier the difficulty of handling the material due to the fine particulate nature of TiO_2 along with a relatively high electrical energy cost because the quantum yield is a bit too low, has limited the commercialization and widespread use of this technology. The technology is commercial in "passive" applications such as self cleaning bathroom tiles in Japan.

1.2.2 Integrated Photocatalyst and Adsorbants

The difficult handling of the fine TiO_2 particles may be solved by depositing the TiO_2 on a surface. If a zeolite, or other absorber, is also present then the organic compound may be adsorbed onto the surface thus reducing the problem of encounter between the organic molecule and the TiO_2 particle from a three dimension problem to a two dimension problem. This allows "pre-concentration" to reduce the electrical energy costs since reaction rates increase with increasing concentration.

The catalyst used for this research is called UCPG204. This catalyst was prepared by mixing degussa P25 TiO_2 with HS-40 colloidal silica. Once the mixture

is homogeneous it is added to glass beads and mixed well. This is dried overnight in a fumehood and then oven dried overnight at 100 °C. Then the catalyst "block" is gently crushed, homogenized, sieved, and washed free of fines. Because the organic content of pulpmill wastes is high, no zeolite is included. However, the silica binder and glass surface do add an appropriate level of adsorption capacity. A zeolite may be used for cases in which more adsorption is needed.

1.3 Pulpmill Waste

1.3.1 Brief History of Pulping

It is well known that Egyptians were the first to produce writing material. They produced this material by pasting together thin layers of the papyrus plant stem (Figure 1.3-1); from which paper gets its name[29].

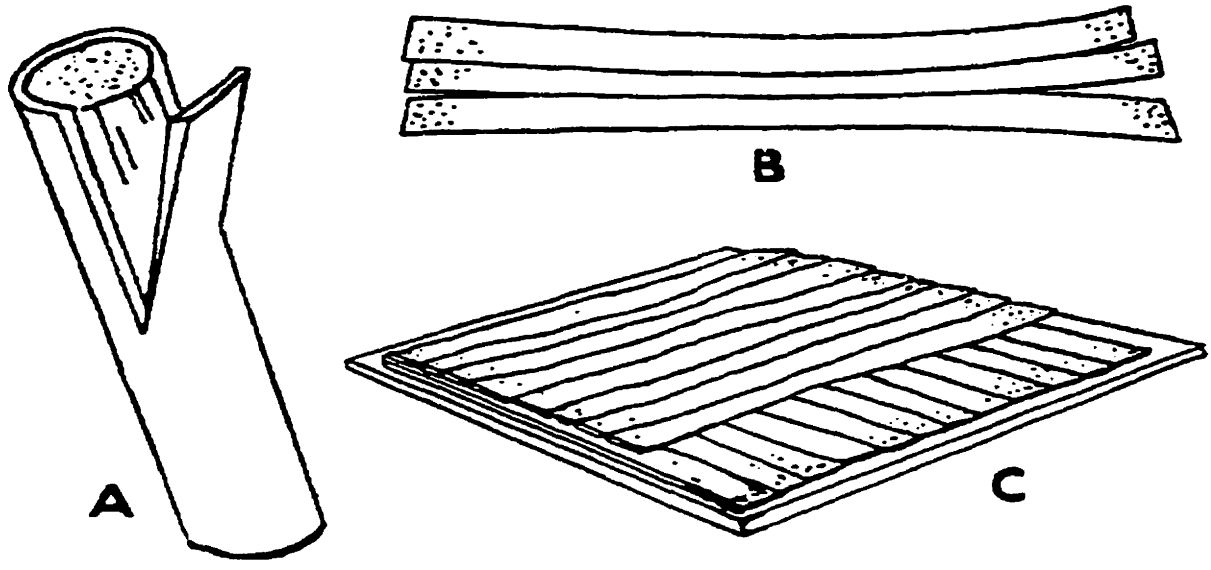

Figure 1.3.1-1: Process of making the Egyptian style writing material
A) The cortex was removed and the pith split into thin strips
B) The strips were then laid in a lattice pattern
C) Then bound into a single sheet. [29]

However, it was the Chinese who developed the first authentic papermaking process. They utilized their method of suspending bamboo or mulberry fibres as early as 100 AD[29].

Several centuries later the knowledge of papermaking reached Europe and the Middle East. These continents used cotton and linen rags to make their paper, and by the 15th century France, Germany, Italy, and Spain had papermills. It wasn't until 1690 that North America had its first papermill located near Philadephia.

In 1798 Nicholas-Louis Robert received a patent for the first continuous papermaking machine. Donkin improved Robert's design in 1807. In 1809 John Dickinson received a patent for the cylinder papermachine which America first had in 1817. America then saw the first Fourdrinier machine in 1827. Mechanical or Groundwood pulping was developed in Germany in 1840; however, it wasn't until

1870 that this process was commercially used. The first manufacture of wood pulp, which was done using the soda process, was in 1854. Benjiman Tilghman received a patent in 1867 for developing the sulfite process, which was first used commercially in 1874. The most widely used pulping process, which is kraft pulping, was developed in 1884 by Carl Dahl. The twentieth century brought along refinement and modification to this technology. There has also been development of techniques like continuous cooking, continuous multistage bleaching, and computer process control.[29]

The processes used from the start of the paper industry to the late 1980's used vasts amounts of water. An 85% reduction in water use came along with the development of closed pulping design (see Figure 1.3-2), which was brought along by the discovery of dioxin emission by pulpmills that occurred in 1985. [30]

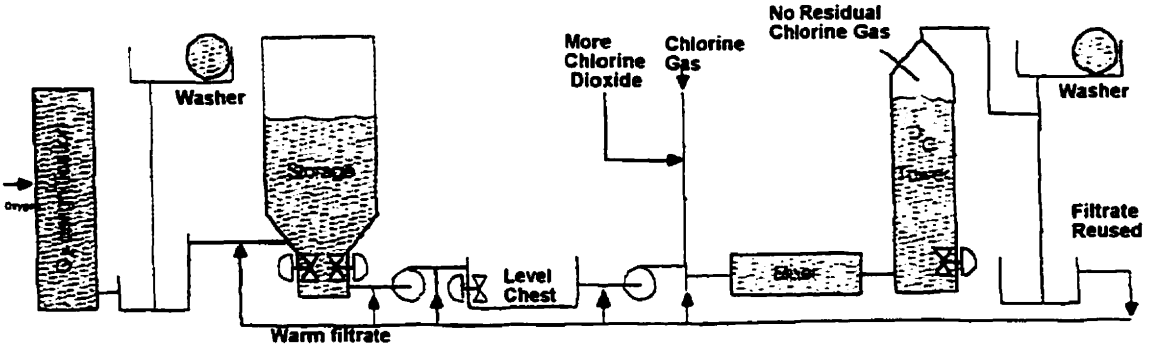

Figure 1.3.1-2: Modern method of pulping, closed pulping where filtrate is recycled and reused.[30]

Along with the need for dioxin reduction and closed pulping came the development of techniques such as continuous cooking, continuous multistep bleaching, and the use of chemicals like hydrogen peroxide and chlorine dioxide (see Figure 1.3.1-2). [30]

1.3.2 Components of Waste Streams

1.3.2.1 Different Classes of Components

Cellulose: Cellulose is found in plant fibres and determines the character of the fibre and enables plant use for making paper[29]. Cellulose is a carbohydrate made up of many glucose units (see Figure1.3.2-1); therefore, it has the ability to form hydrogen bonds and so has an affinity to water. The strength of the paper sheet comes from the hydrogen bonds between two cellulose molecules[29][30].

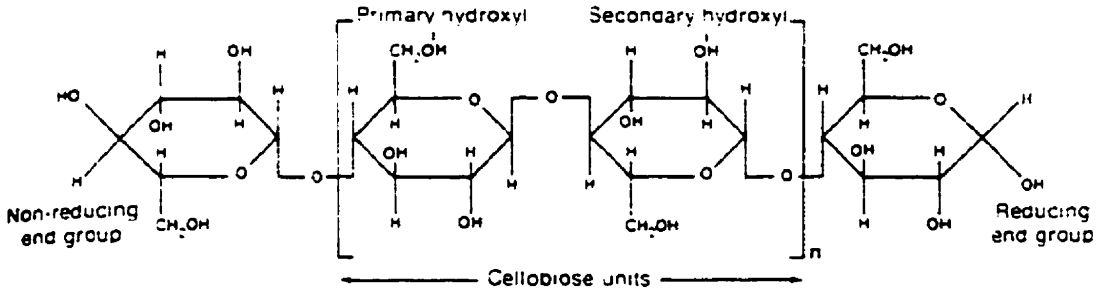

Figure 1.3.2-1: Cellulose molecule

Hemicellulose: Hemicellulose contains five different sugar units (glucose, mannose, galactose, xylose, and arabinose) [29]. Some of the hemicellulose molecules will be more closely related in a structural manner to cellulose while others will be more closely related in a structural manner to lignin[29]. Upon caustic treatment, or kraft cooking, hemicellulose is easily degraded and dissolved, due to

its difference in structure from cellulose, resulting in a lower percentage of hemicellulose in the pulp than in the wood[29][30].

Lignin: Lignin is an amorphous highly polymerized substance[29]. Its building blocks are phenylpropane units arranged in a random 3-D formation[30] (see Figure 1.3.2-2). Hydrolysis of the wood lignin bond takes place during kraft pulping; thus, decreasing weight, causing dissolution, and removing the lignin without damaging the cellulose fibres[30].

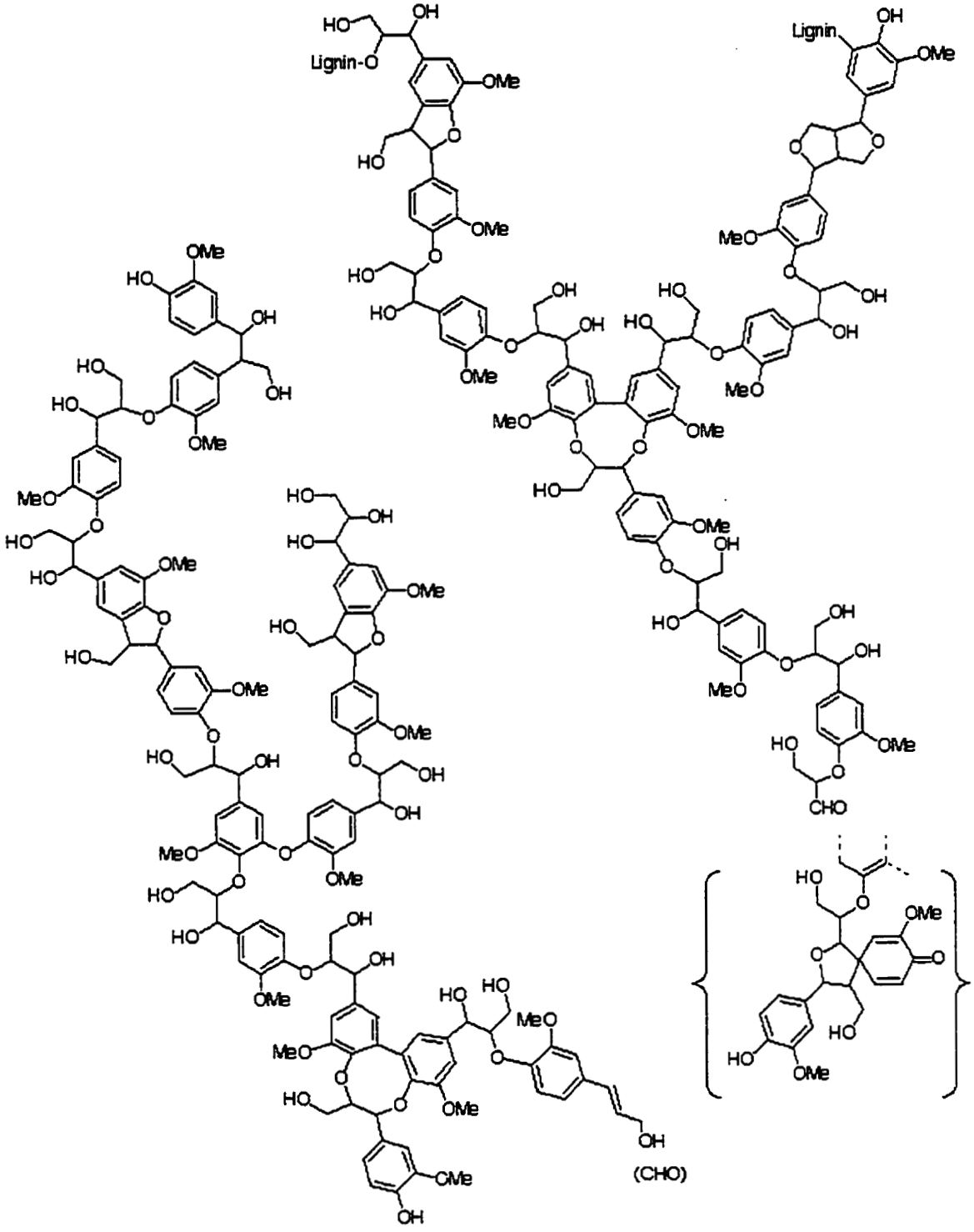

Figure 1.3.2-2 structure of softwood lignin[35]

Extractives: Extractives are substances such as resin acids, fatty acids, terpenoid compounds, and alcohols which may be present in the native fibres of the plant source(see Figure 1.3.2-3). Most of these substances are soluble in water or neutral organic solvents.[30][31]

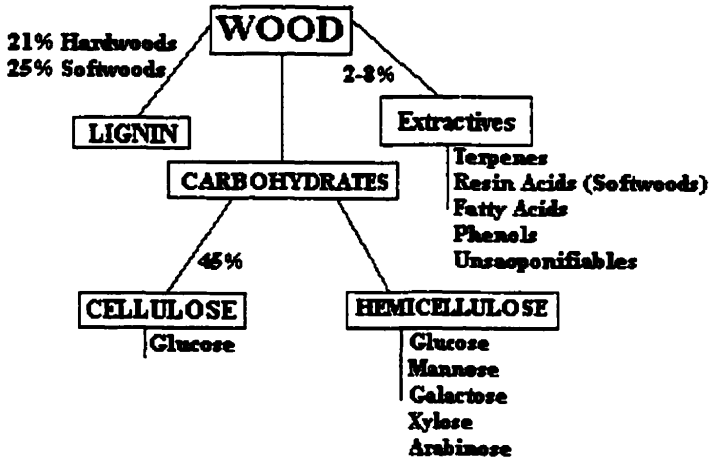

Figure 1.3.2-3: Source of extractives found in wood.[29]

1.3.2.2 Components of Environmental Concern

Since pulpmills discharge their treated wastewater into the surrounding bodies of water; the impact of this waste to the ecosystem and living organisms is important and guidelines for the wastewater discharge are getting more stringent.

Resin acids have been shown to contribute to the toxicity of the discharged effluent. They are toxic to a number of living organisms and the acute lethal concentration to rainbow trout is 0.4-1.1 mg/L[32], [31].

It is known that medium length chain triglycerides are toxic to animals and humans. The major worry being that if people consume any fish or animal that has been exposed to these triglycerides they can be transferred from fish to humans upon consumption of the fish.[40]

Fatty acids are not water soluble and so can easily be removed; however, lipophilic extractives may be slightly water soluble and cause pitch deposits on the paper machine, specks in the paper, decrease wet strength, interfere with cationic process chemicals, and impair sheet brightness. [31]

Although the lignans (which are short-chain lignins) from the leaves, seedlings and micropropagated plants of *Rollinia mucosa* (Jacq.) Bail have been known to be used in the treatment of tumors in the West Indies and Indonesia[33]; it has been found that the lignans from kraft pulp from North American sources cause pitch deposits on the paper machine and cause paper to yellow over time[29][30][31].

1.3.2.3 Regulatory Parameters for Discharge

Following the 1980's finding of dioxins being contained in the discharge of pulpmill wastewaters there have been more stringent regulations on wastewater discharge. This has not only been on the part of the government. The pulp and paper industry have been willing to take part in research concerning all of their wastes and improvement of the pulping technology, and for better and more effective treatment of the effluents.[30]

The guidelines for discharge concerning the components studied in this research and found in pulpmill wastewaters are outlined in Table 1.3.2-1. It should be noted that these guidelines are for the province of Alberta and that each province has its own guidelines although some may be similar.

Aesthetically the wastewater should be free from materials that will settle and form harmful deposits, floating debris, oil, scum, and other unappealing matter; substances increasing colour, odour, taste, or turbidity; and substances that can be harmful to the aquatic life when combined with other substances, or in the right conditions, are toxic on their own [34]. The guidelines for the colour of the effluent is that it must not increase the colour of the receiving waters by more than 30 colour units[34]. Colour units are determined by a visual comparison of the sample with known concentrations of platinum-cobalt solutions [39]. One colour unit is determined to be a platinum solution of 1mg/Lmade from chloroplatinate ion. The ratio of cobalt to platinum may be varied to match the hue of the sample.

$$\text{Colour units} = \frac{A \times 50}{B} \quad [39] \quad (1.3.3\text{-}1)$$

Where A is the estimated colour of the diluted sample and B is the sample volume in mL used.

The threshold odour number (TON) at 20°C must not exceed 8[34]. The threshold odour number is determined by comparing the smell of samples of various degrees of dilution to an odour free water [39]. The degree of dilution of the most diluted water sample is used to calculate the threshold odour number.

$$TON = \frac{A + B}{B} \quad [39] \qquad (1.3.3\text{-}2)$$

A= volume of sample in mL
B= volume of odour free water used for dilution in mL

Sample Volume	
Diluted to 200 ml	TON
200	1
140	1.4
100	2
35	6
17	12
4	50
1.4	140
1	200

Table 1.3.3-1 Sample threshold odour numbers

Substance or Conditon	Category	unit	Alberta		CCME	USEPA	
			Acute	Chronic		Maximum	Continuous
Alkalinity (as $CaCO_3$)	Ions and General	mg/L					20
Chloride	Ions and General	mg/L				860	230
Chlorine	Ions and General	µg/L			0.5	19	11
Chloroform	Trace Organic	µg/L			1.8		
Chlorophenol (mono)	Trace Organic	µg/L			7		
Chlorophenol (di)	Trace Organic	µg/L			0.2		
Chlorophenol (tri)	Trace Organic	µg/L			1.8		
Chlorophenol (tetra)	Trace Organic	µg/L			1		
Cholophenol (penta)	Trace Organic	µg/L			0.5	19	15
Phenoxy herbicides	Pesticide	µg/L			4		
Chlorothalonil	Pesticide	µg/L			0.18		
Chloropyrifos	Pesticide	µg/L			0.0035	0.083	0.041
DDT	Pesticide	µg/L				1.1	0.001
1,2-Dichlorobenzene	Trace Organic	µg/L			0.7		
1,3-Dichlorobenzene	Trace Organic	µg/L			150		
1,4-Dichlorobenzene	Trace Organic	µg/L			26		
1,2-Dichloroethane	Trace Organic	µg/L			100		
DDAC	Pesticide	µg/L			1.5		
Di-n-butyl phthalate	Trace Organic	µg/L			19		
Di(2-ethylhexyl)phthalate	Trace Organic	µg/L			16		
Ethylene glycol	Trace Organic	µg/L			192000		
Nitrigen (total)	Nutrient	mg/L		1			
Dissolved Oxygen	Ions and General	mg/L	5.0(1-day min)	6.5(7-day mean)	5.5-9.5	3.0-9.5	
PCBs	Trace Organic	µg/L					0.014
Pentachlorobenzene	Trace Organic	µg/L			6		
pH	Ions and General		6.5-8.5[a]	6.5 8.5[a]	6.5-9.0		6.5-9.0
Phenanthrene	Trace Organic	µg/L			0.4		
Phenolics	Trace Organic	µg/L		5			
Phenols(mono and dihydric)	Trace Organic	µg/L			4		
Propylene glycol	Trace Organic	µg/L			500000		
Resin acids	Trace Organic	µg/L		100			
Sulphide (H_2S)	Ions and General	µg/L					2
1,2,3,4-Tetrachlorobenzene	Trace Organic	µg/L			1.8		
1,1,2,2-Tetrachloroethelyne	Trace Organic	µg/L			111		
Tributyltin	Trace Organic	µg/L			0.008	0.46	0.063
1,2,4-Trichlorobenzene	Trace Organic	µg/L			24		
1,2,3-Trichlorobenzene	Trace Organic	µg/L			8		
1,1,2-Trichloroethene	Trace Organic	µg/L			21		
Triphenyltin	Trace Organic	µg/L			0.022		

Table 1.3.3-2- regulatory parameters for pulpmill waste emissions for the protection of fresh water aquatic life[34] a) must not alter the pH more than 0.5 pH units from background value

The clarity of the water should be at a level where a Secchi disc is visible at 1.2 m. A Secchi disc is a device used to measure the degree of light penetration through a body of water. The degree of light penetration indicates quantities of

suspended material in the water. Suspended particles may be inorganic, such as silt, or of an organic origin, such as plant matter. [38]

The turbidity of the whitewater should not increase the turbidity of the receiving water by 5.0 NTU[34]. The nephelometric turbidity units are based on a comparison of intensity of scattered light by the measured sample under specific conditions[39]. The reference suspension is made from formazin polymer; it is easy to prepare and has reproducible light scattering properties. A specified concentration of the formazin suspension has a defined turbidity of 40 NTU. The nephelometric turbidity units are calculated from the following formula:

$$NTU = \frac{A \times (B + C)}{C} \quad [39] \qquad (1.3.3\text{-}3)$$

Where A is NTU found in the dilute sample, B is the volume of water used for dilution in mL, and C is volume of sample used for the dilution.

The temperature of the wastewater should not increase or decrease drastically deep body temperatures of bathers[34].

There are many factors that affect the guidelines. For example, in the case where effluent is almost instantaneously dispersed the guidelines would be applicable near the end of pipe rather than at the edge of a defined mixing zone[34].

1.4 Past Observations on Photocatalytic Treatment of Pulpmill Streams

Previous work done with a similar photocatalyst to the one used in these studies and with a "rotating tube" reactor, as opposed to the fluidized bed reactor

used in these studies, has shown that supported TiO_2 is effective in degrading the major components of whitewater: dissolved organic matter and colloidal organic matter. The main difference between treatment by direct photolysis, treatment with degussa P25 TiO_2 and a supported TiO_2 was the pathway in which the photocatalysis occurred.

The photocatalytic treatments were monitored by High Pressure Liquid Chromatography. However, the individual peaks were not assigned , the change in peak size was monitored. Intermediates were defined only by their retention time and by the fact that they were not present in the beginning, but appeared during treatment. Because HPLC was used only as a monitoring device an extensive analysis was done at UBC on a sample whitewater to confirm the findings; results are outlined in Table 1.4-1.

	Whitewater	Treatments		
Parameter	Mill WW	UC 210	UC210+HP	HP
Dissolved and colloidal solids C mg/L	2360	1120	160	340
Lignin, mg/L	100	80	15	7.5
Ash mg/L	390	213	67	163
Carbohydrate mg/L	1560	670	Not detected	Not detected
	EXTRACTIVES			
Resin and Fatty Acids mg/L	14	20.5	15.4	58.3
Sterol and Lignan mg/L	88	34.3	16.4	26.6
Steryl Esters and Triglycerides mg/L	16	12.3	9.9	11.3

Table 1.4-1: Previous results of treatments on wastewater, extensive analysis done at UBC. The amount of hydrogen peroxide added was 1% H_2O_2 v/v

It was observed that there was a successive decrease in the more non-polar aromatics and an increase in the more polar aromatics compared to the original whitewater solution. This was found to be due to the fact that as the photocatalysis takes place the non-polar aromatics are first hydroxylated and then broken down and some ring opening takes place. Aromatics "move" from one class to another.

As in this research, there have been some comparative studies of the catalytic ability of the photocatalysts. These suggested that there was minimal breakdown with direct photolysis; however conversion was improved with the supported TiO_2 and the formation of an intermediate that does not arise during direct photolysis. This suggests that the oxidation occurs by a different pathway than that of direct photolysis. It was also observed that when hydrogen peroxide was added to the photocatalyst, the same intermediate was observed as when the catalyst was used; however, the intermediate was formed more rapidly. The addition of hydrogen peroxide also caused a significant increase in rate of breakdown of the initial components. After six days of irradiation there were only trace amounts left. When degussa P25 TiO_2 was used in a comparison to the catalyst there was no evidence of the intermediates being formed, again when hydrogen peroxide was combined with the degussa P25 TiO_2 the intermediates were once again formed and subsequently decomposed. This suggests that the degradation occurs via the same pathway as with the composite catalyst. Interestingly, it also appears that the addition of hydrogen peroxide only affects the initial rate of photocatalytic breakdown by providing extra $\cdot OH$ radicals to the

solution. Providing a continuous source of hydrogen peroxide during the treatment had no apparent effect on the rate of breakdown. H_2O_2 appears to be an initiator for starting the organic chain reactions.

1.5 Goals of Project

1.5.1 Goal of Simplified Analysis

In order to monitor performance of pilot scale and production photoreactors, practical rapid analysis is required. Pulpmill streams are complex mixtures. The present methods of analysis like the one out lined below in Figure 1.5-1 are time consuming and complex and therefore inappropriate for routine analysis. Hence, a rapid method for routine analysis applications is needed.

Our proposal is to monitor performance by conducting a "crude" analysis starting from a MTBE extraction from the aqueous stream followed by HPLC analysis of organic and aqueous phases supplemented as appropriate by UV-vis spectrometry. The objectives are to recognize changes in initial substrate concentrations, recognize partial oxidation intermediates, and determine the ultimate degree of mineralization. Clearly, it will not be possible to identify individual compounds during near "on-line" performance monitoring. The approach will be to quantify some model compounds and approximate

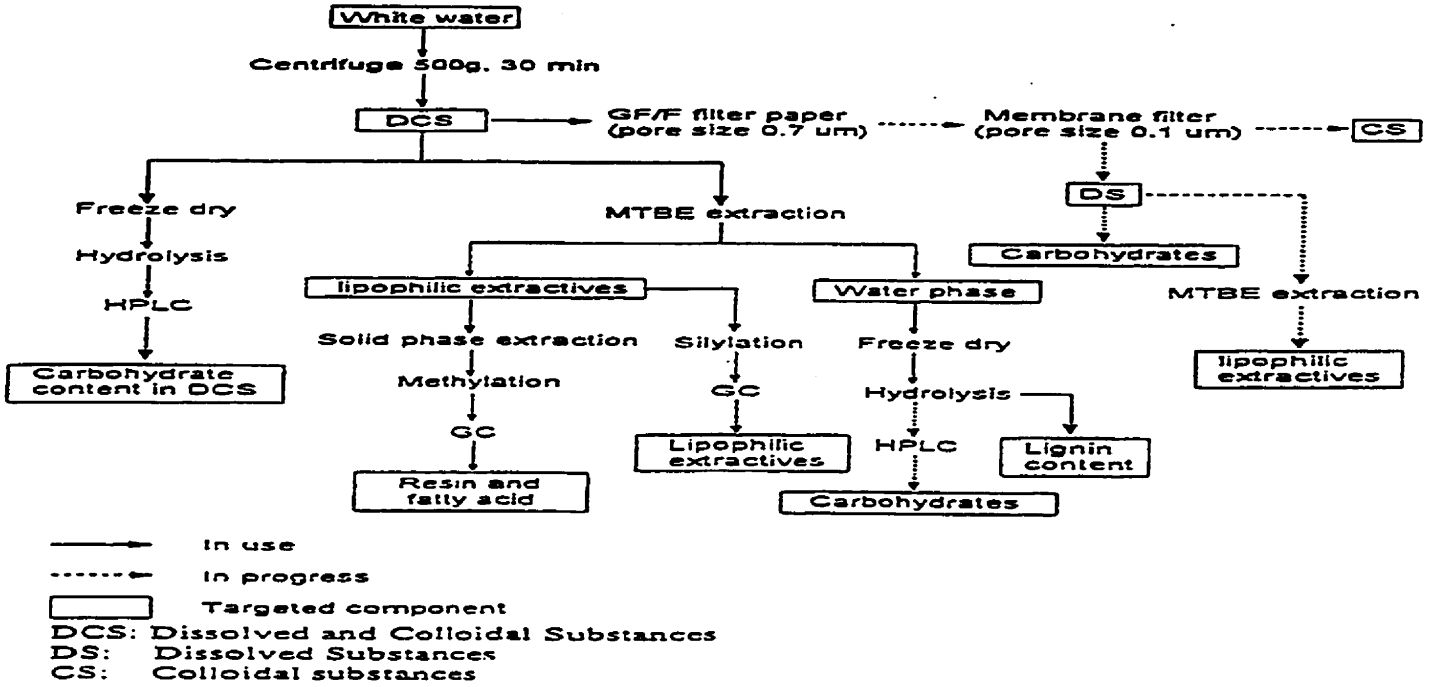

Figure. 1.5-1. Present method for extraction of target compounds for analysis used by the department of Forest Products Biotechnology at the University of British Columbia. This method has been estimated to take two days to perform.

concentrations by assuming that the model are close in HPLC sensitivity to other compounds with the same chromophores (UV detection is used). UV-visible spectrometry is also used to verify if intermediates having absorption at different wavelengths than the one used in HPLC chromatography are being formed.

The chromatographic separations will serve to segregate major classes of the organic components of the stream to a reasonable approximation. The result is expected to be a semi-quantitative monitor that becomes more specific and precise as total mineralization is approached.

1.5.2 Goal of Establishing Relative Efficiency of Different Component Oxidation

Since it is the overall oxidation of the various components that will determine the gross effectiveness of photochemical treatment of pulpmill streams, it is important to understand the relative rates of reaction and relative complexity of pathways for each of the major groups. As well, it is useful to recognize that some compounds will undergo direct photolysis under UV irradiation and the relative efficiency of such pathways merits investigation. Also, traditionally UV-H_2O_2 has been an accepted homogeneous method of photooxidation[3] and H_2O_2 has been observed to promote TiO_2 photocatalyzed systems. Thus, the effect of added H_2O_2 merits attention. Finally, Degussa P25 TiO_2 is the most widely studied TiO_2 photocatalyst[4]. It is useful to compare our supported TiO_2 materials to Degussa P25 TiO_2.

References

1. Sustainable Forest Management. UBC reports #2 and #3.

2. Vaisman, Elena, Cook, Robert, L., Langford, Cooper, H., *J. Phys. Chem. B.*, **2000**, 8679-8684.

3. Calvert, J. G., Pitts Jr., J. N., "Photochemistry", John Wiley and Sons, New York, **1966**.

4. Boehm, H.P., *Faraday Diss.*, **1971**, 264-275.

5. Patrick, T.B., Bechtold, D.S., *J.Org. Chem.*, **1984**, 1935-1937.

6. Yokota,T., Yashima, K., Takigawa, T., Takahashi, K., *J. Chem. Eng. Japan*, (24), 5, **1991**, 558-562.

7. Yokota,T., Yashima, K., Takigawa, T., Takahashi, K., *J. Chem. Eng. Japan*, (22), 5, **1989**, 543-548.

8. Pouliquen, J., Wintgens, V., et al, *Can. J. Chem.*, (62), **1984**, 2478-2486.

9. Schendiman, D.P., and Kutal, C., *J. Am. Chem. Soc.*, (99), 17, **1977**, 5677-5682.

10. Padwa, A., Pulwer, M.J., Rosenthal, R.J., *J.Org. Chem.*, (49), **1984**, 856-862.

11. Friesen, D.A., Morello, L., Headley, J.V., Langford, C.H., *J. Photochemistry and Photobiology*, (133), **2000**, 213-220.

12. Friesen, D.A., Gibson, D.B., Langford, C.H., *Chem Commun.*, **1998**, 543-544.

13. Bigda, R.J., *Chemical Engineering Progress.*, **1995**, 62-66.

14. Barreto, R.D., Gray, K.A., Anders, K., *Wat. Res.*, (29), 5, **1995**, 1243-1248.

15. Liu, G., Li, X., Zhao, J., *Environ. Sci. Technol.*, (34), **2000**, 3982-3990.

16. Lichtin, N.N., Dong, J., Vijayakumar, K.M., *Water Poll. Res. J. Canada*, (27), 1, **1992**, 203-210.

17. Ollis, D.F., Pelizzetti, E., Serpone, N., *Environ. Sci. Technol.*, (25), 9, **1991**, 1523-1529.

18. Hoffmann, M.R., Martin, S.T., Choi, W., Bahnemann, D.W., *Chem Rev.*, (95), **1995**, 69-96.

19. Lichtin, N.N, Muthusami, A., Berman, E., Dong, J., *Res. Chem. Intermed.*, (20), 7, **1994**, 755-781.

20. Lichtin, N.N., Avudaithai, M., Berman, E., Grayfer, A., *Solar Energy*, (56), **1996**, 377-385.

21. Mozzanega, H., Herrmann, J.-M., Pichat, P., *J. Phys. Chem.*, (83), 17, **1979**, 2251-2255.

22. Amenomiya, Y., *Journal of Catalysis*, (46), **1977**, 326-339.

23. Moffat, J.B., and Neelman, J.F., *Journal of Catalysis*, (39), **1975**, 419-431.

24. Bielanski, A., Datka, J., *Journal of Catalysis*, (32), **1974**, 183-189.

25. Bickley, R.I., Stone, F.S., *Journal of Catalysis*, (31), **1973**, 389-397.

26. Djeghri, N., Formenti, M., Juillet, F., Teichner, S.J., *Faraday Diss.*, (74), **1974**, 185-193.

27. Rivas, F.J., Beltran, F.J., Gimeno, O., Frades, J., *J. Agric. Food Chem.*, (49), **2001**, 1873-1880.

28. Plotnikov, J., "Allgemeine Photochemie," 2nd ed., Walter de Gruyter, West Berlin, 1936.

29. Smook, G.A. "Handbook for Pulp & Paper Technologists," Canadian Pulp and Paper Association, Montreal, Canada, 1984.

30. Ferguson, Kelly, "Environmental Solutions for the Pulp and Paper Industry," Miller Freeman Incorporated, San Francisco, 1991.

31. Orsa, F., Holmbom, B., *J. Pulp and Paper Science*, (20), **1994**, J361-J366.

32. Peng, G., Roberts, J.C., *Water Research*, (34), **2000**, 2779-2785.

33. Figureueiredo, Solange, Faria, Lua, Viana, Vera, Regina, Campos, Simoes, Claudia, Albarello, Norma, Trugo, Luiz, Carlos, Kaplan, Maria, Auxiliadora, Coelho, Krul, William, Robert, *Plant Cell, Tissue and Organ Culture,* (56), **1999**, 121-124.

34. Alberta Environment, Environmental Service Environmental Sciences Division, Natural Resources Service Water Management Division, Surface Water Quality Guidelines for Use in Alberta, Pub. No T/483, ISBN 0-7785-0897-8, **1999**, 1-20.

35. Gösta Brunow, Jussi Sipilä, Pirkko Karhunen, http://www.helsinki.fi/~orgkm_ww/lignin_structure.htmL; last accessed August 7, 2001

36. Fugishima, A., Honda, K., *Nature (London),* (238), **1972**, 37-38.

37. Carey, J. H., Oliver, B. G., *Nature (London),* (259), **1976**, 554-556.

38. Carlson, R.E. and J. Simpson, "A Coordinator's Guide to Volunteer Lake Monitoring Methods" North American Lake Management Society, 96, 1996.

39. APHA, AWWA, WPCE, "Standard Methods For the Examination of Water and WasteWater", 15thed, American Public Health Association, Washington DC, 60-63, 80-83, 132-134, 1980.

40. Traul, K. A., Driedger, A., Ingle, D. L., Nakhasi, D., *Food and Chemical Toxicology,* **2000**, 79-98.

2 Experimental

2.1 Materials

The chemicals used to represent the target compounds in the model whitewater are: vinyl acetic acid with a purity of 97% to represent the fatty acids, abietic acid with a purity of 70% to represent the resin acids, ethyl nonanoate with a purity of 97% to represent the steryl esters, lignin alkali was chosen to represent the lignins. All of these compounds were purchased from Aldrich. Triacetin, with a purity of 99% was used to represent triglycerides. It was purchased from Sigma.

The catalyst used for the photocatalytic breakdown of the target compounds was UCPG204 pill. The effectiveness of the catalyst was compared to degussa TiO_2. The preparation of this catalyst is described in section 2.2.2. Crystals of $K_3[Fe^{III}(C_2O_4)_3]\cdot 3H_20$ used in the light intensity measurements described below were prepared by combining 3 volumes 1.5 M potassium oxalate solution and one volume of 1.5 M ferric chloride aqueous solution.

$$3K_2(C_2O_4) + FeCl_3 \rightarrow K_3Fe(C_2O_4)_3 + 3KCl \qquad (2.1)$$

The resulting mixture was left to stand in the dark for a few days. Large green $K_3[Fe^{III}(C_2O_4)_3]\cdot 3H_20$ crystals precipitated out. The $K_3[Fe^{III}(C_2O_4)_3]\cdot 3H_20$ crystals were then recrystallized four times from warm deionized water then oven dried at 40°C. The product yield was 75%. [1],[2]

2.2 Analytical procedures

The instrument used for the HPLC analysis was a Waters 600 controller and solvent delivery system with a 486 tuneable absorbance detector with deuterium lamp. The instrument used for the UV-visible analysis was a Hewlett Packard model 8552A diode array spectrophotometer interfaced to a PC computer.

10 mL aliquots of irradiated target compounds were extracted with three 10mL portions of *tert*-butylmethylether, dried over anhydrous sodium sulfate, and then gravimetrically filtered through number 2 Whatman filter paper. They were then analysed with HPLC using UV-visible detection at a wavelength of 230 nm; the detection limit was 1×10^{-7} M for vinyl acetic acid, 1×10^{-5}.for abietic acid, 1×10^{-4} for ethylnonanoate, 100 ppm for lignin alkali, and 1×10^{-4} for triacetin.

The column used for the HPLC analysis was a discovery C-18 column (purchased from Supleco), the column length is 25 cm, diameter is 4 mm, and packing material diameter is 5 μm. The mobile phase used was 1% tris buffer (pH 7), 74% deionised water (at pH 7), and 25% acetonitrile. Detection was done at 230 nm, and the flow rate was 1 mL/min. In order to detect the ethylnonanoate the mobile phase was changed to 24% deionised water, 75% acetonitrile, and 1% tris buffer; the wavelength was also changed to 240 nm. UV-visible spectrometry was also used to see if intermediates absorbing at different wavelengths were formed.

2.3 Photocatalytic Procedures

2.3 Photocatalytic Procedures

2.3.1 Reactor Description

The reactor used consists of a 10 mL quartz tube immersed within 16 lamps of wavelength range of 315-380 nm. The reactor is a fluidized bed reactor that can be used in a two stage adsorption/regeneration process to handle large flow rates of streams to be treated. It enhances contact efficiency since the reaction rate of photoreactor processes is directly affected by the flow rate. Moreover each catalyst particle is equally irradiated.

2.3.2 Oxidation Procedures

Stock solutions of each representative chemical were prepared in methanol. A 10 mL aliquot was then taken and diluted to 100 mL with deionized water. This resulting solution, which is slightly acidic, was then irradiated for a 24-hour period; the mixing chamber was open to air during irradiation.

The photocatalytic efficiency was monitored by four different runs. These were: (1) direct photolysis, (2) photolysis with catalyst, (3) photolysis with catalyst and hydrogen peroxide, and (4) photolysis with Degussa P25 titanium dioxide. Samples of the irradiated target compound were taken at the start (after one hour of equilibration in the reactor system where the solution was pumped through the

reactor in the dark), for 1 hour of irradiation, for 4 hours of irradiation, for 20 hours of irradiation, and for 24 hours of irradiation.

For compounds which were oxidized photolytically more efficiently then by photocatalysis, a second set of runs was performed. These runs were started by an initial 24-hour irradiation period (run #1), after which either run #2, #3, or #4 was performed. For these runs, samples were taken at the start (after one hour of equilibration in the reactor system where the solution was pumped through the reactor in the dark), 5 hours of irradiation, 24 hours of irradiation, 29 hours of irradiation, and 48 hours of irradiation. These times were chosen in order to monitor the formation and breakdown of intermediates. These samples were then analyzed by the aforementioned procedure.

2.3.3 Light Intensity Measurements by Ferrioxalate Acinometry

Throughout the experiments the light intensity entering the reaction chamber from the lamps was measured. The procedure used to measure the light intensity was solution chemical actinometry. The most reliable and most widely used solution chemical actinometer for the near UV is the potassium ferrioxilate system[1], which was developed by Parker and Hatchard[2]. This actinometer has good sensitivity for wavelengths which range from 254 nm to more than 400 nm.

When potassium ferrioxalate, $K_3[Fe^{III}(C_2O_4)_3]\cdot 3H_20$, is irradiated the Fe^{III} is converted to Fe^{II} (ferrous ion). The amount of ferrous ion produced can determined by UV-visible spectrometry following complexation with 1,10-phenanthroline

(*phen*). The resulting chelate $[Fe^{II}(phen)_3]^{2+}$ is red and has a maximum absorption at a wavelength of 510 nm. From the absorbance one can calculate the moles and number of ferrous ions formed during irradiation (N_{Fe}^{II}/s). Knowing the number of ferrous ions formed one can determine the number of photons/s (I), the light intensity, using equation 2.3-1

$$N_{Fe}^{II}/s = (V_1 \cdot V_3 \cdot N_A \cdot A_{510})/(V_2 \cdot \varepsilon_{Fe}^{II} \cdot t \cdot l) \qquad (2.3\text{-}1)$$

Where V_1 is the volume of irradiated actinometer solution;

V_2 is the volume of the aliquot taken for analysis;

V_3 is the volume of the flask in which the aliquot is diluted;

N_A is Avogadro's number;

A_{510} is absorbance of $[Fe^{II}(phen)_3]^{2+}$ at 510 nm;

ε_{Fe}^{II} is molar extinction coefficient of Fe^{II} complex

$(1.11X10^4$ L/mole cm);[1]

t (s) is the time of irradiation;

l is the path length (1 cm)

Calculation of the light intensity, I, was done according to equation 2.3-2

$$I \text{ (photons/s)} = (N_{Fe}^{II}/sec)/(\phi_{Fe}^{II} \cdot I_f) \qquad (2.3\text{-}2)$$

where ϕ_{Fe}^{II} is a quantum yield for the formation of Fe^{II}; which is 1.21 near 350 nm, and I_f is a fraction of the light absorbed by the actinometer which is 1.0 for

wavelengths below 400 nm. The 7.63×10^{-3} molar concentration of the actinometer compound used was sufficient to absorb all the entering light. This was confirmed by the lack of change in light intensity with change in concentration of the irradiated potassium ferrioxalate solution.

The aqueous solutions required to carry out a light intensity measurement are:

1. 0.1% (w) 1,10- phenanthroline which is stored in the dark to prevent photodecomposition of the phenanthroline
2. sodium acetate buffer: 41 g sodium acetate, 5 mL conc. H_2SO_4 diluted to 500 mL with deionized water
3. a 7.63×10^{-3} M ferrioxalate solution in 0.1 N H_2SO_4 prepared in the dark

For the measurements made, 5 mL of ferrioxalate solution was irradiated. A 3.00 mL aliquot of irradiated ferrioxalate solution was quantitatively transferred into a 50.00 mL volumetric flask containing 1.5 mL of sodium acetate buffer, 6 mL of 1,10-phenanthroline solution was added, and then diluted to the mark with deionised water. The resulting solution was placed in the dark to develop for one hour. The absorbance of the resulting complex was measured by UV-visible spectrometry.

For our purposes, a comparison to solar irradiation is interesting. The equivalent sunlight hours can be calculated from the intensity[5]. To calculate the number of lamp hours equivalent to sunlight hours the number of photons/s of sunlight was estimated using equation (2.3-3). To do so it was assumed that the

sunlight irradiated straight through the atmosphere to the reactor, air mass 1, and that the wavelengths which are photocatalytically active range from 330 nm to 380 nm. Once the photons/s of sunlight is known the ratio of photons/s_{sun} to photons/s_{lamp} is then calculated, the result is then multiplied by the amount of seconds in a 24 hour period. Since the reactor used is a flow through reactor the number of equivalent sunlight hours is multiplied by the ratio volume irradiated to total volume of the reactor plus the reservoir.

$$N = \lambda P/(hc) \qquad (2.3\text{-}3)$$

Where N is the number of photons/s

λ is the wavelength in meters

P is the power in J/s

h is Plank's constant

c is the speed of light in m/s

For our system is was found that approximately 1.2 hours of irradiation was equivalent to 24 hours of sunlight.

References

1. Calvert, J. G., and Pitts, J. N. Jr., "Photochemistry", **1966**, 783-786.

2. Hatcherd, C. G., and Parker, C. A., *Proc. Roy. Soc.*, **1956**, A235, 518.

3. Vaisman, E, M.Sc. Thesis University of Calgary, **1999**, 78-80.

4. Atkins, P., "Physical Chemistry," 5th ed., Oxford University Press, Toronto, **1994**, 366.

5. Duffie, John, A., Beckman, William, A., "Solar Energy Thermal Processes," John Wiley & Sons, New York, **1974**.

6. Chow, S. Z., Shepard, D., *TAPPI Journal*, **1996**, 79, 173-179.

3 Results

As stated in chapter 2 the HPLC analysis was performed on a discovery C18 column. The wavelength was 230 nm for 0 to 9 min and 240 nm for 9 to 25 min. The mobile phase consisted of 25% acetonitrile, 1% tris buffer, and 74% water for 0 to 10 min and 75% acetonitrile, 1% tris buffer, and 24% water for 10 min to 25 min.

The peaks were assigned by running an initial HPLC analysis of the pure compound in MTBE. The analysis of each run was then performed. Peaks which were not seen in the HPLC chromatogram of the pure compound were assigned to be intermediates. The intermediate peaks were observed to "grow" overtime, and in the runs containing hydrogen peroxide, in some cases, they were also observed to decrease in size. Intermediate peaks were assigned, where possible, on their retention time. The concentration of the model compound was calculated by correlation of the peak area with a calibration curve of the compound.

A relative percent reduction was calculated with the following formula:

$$\text{Reduction} = \frac{\text{concentration at start - ceoncentration at 24 hours}}{\text{concentration at start}} \times 100 \quad (3.1)$$

This formula was used to enable comparison between each individual run for a sample.

3.1 Fatty Acids and Resin Acids

As mentioned in chapter 2 the model compound chosen to represent the fatty acids is vinyl acetic acid. It can be detected by HPLC at a wavelength of 230 nm with a mobile phase of 74% water, 1% tris buffer, and 25% acetonitrile, its retention time is approximately 5 min (Figure 3.1-1).

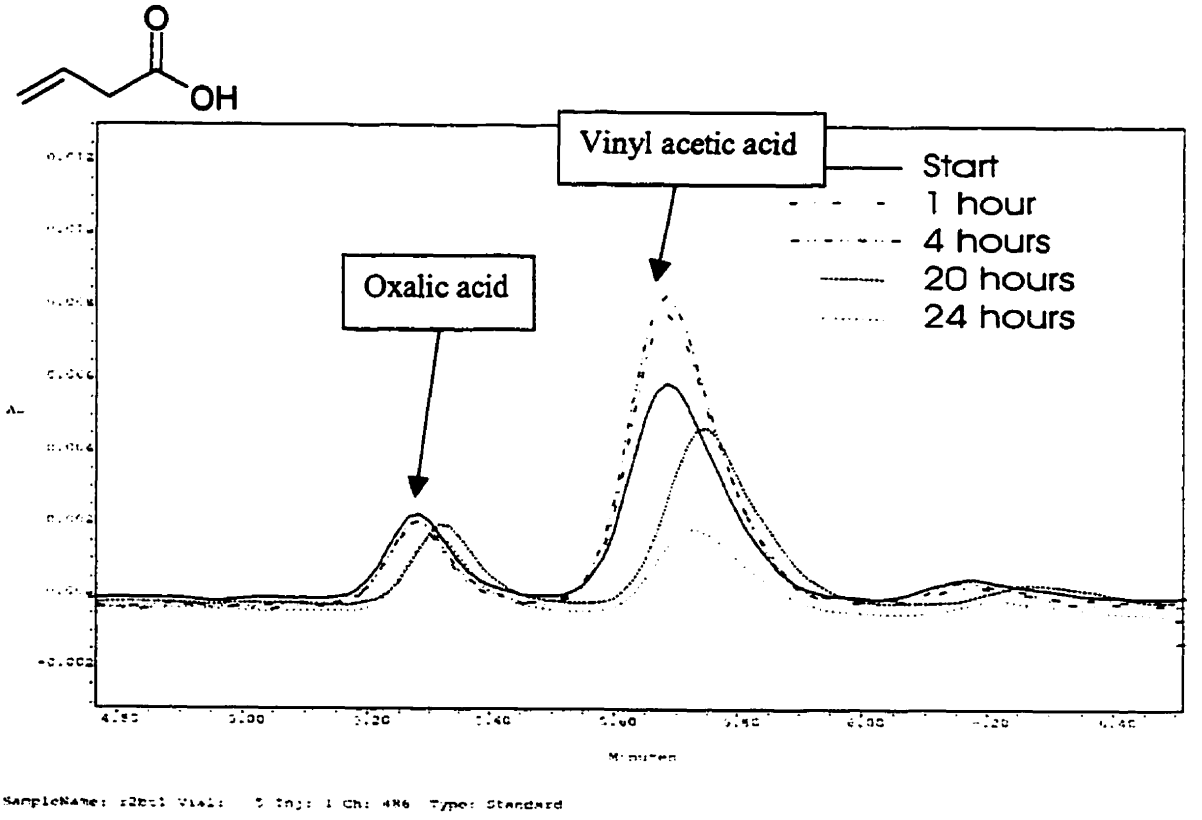

Figure 3.1-1: HPLC chromatogram for vinyl acetic acid. Treatment with supported catalyst. Change from shorter retention time to slightly longer retention time is due to the change in pH from more acidic to less acidic as the degradation takes place.

The intermediates formed during photocatalytic treatment are thought to be formaldehyde and oxalic acid. The intermediates were assigned by retention time; these were verified by comparison with HPLC chromatograms of pure formaldehyde and oxalic acid.

Correlating the peak area with a calibration curve suggests that the different methods of treatment have yielded the results outlined in Table 3.1-1. Vinyl acetic acid is the easiest and fastest component to breakdown. We can see that the addition of hydrogen peroxide helps initiate the oxidation of the organic compounds and as a result the breakdown is over after a relatively short time. We see that treatment with degussa P25 TiO_2 is less effective than the supported catalyst. This is because the degussa P25 TiO_2 surface is hydrolyzed in water and so cannot adsorb organic compounds well. However when supported on a glass surface by silica, the silica adsorbs the organic compound and the TiO_2 is rendered effective. It is predicted that for real water treatment there will be vinyl acetic acid present for longer times because there will be some produced from larger molecules as they are being broken down.

UV only			UV & catalyst	
Time	Conc (M)		Time	Conc (M)
Start	$1.45 \pm 0.05 \times 10^{-2}$		Start	$1.15 \pm 0.03 \times 10^{-2}$
1 hr	$1.93 \pm 0.05 \times 10^{-2}$		1 hr	$1.32 \pm 0.02 \times 10^{-2}$
4 hr	$2.00 \pm 0.09 \times 10^{-2}$		4 hr	$1.29 \pm 0.04 \times 10^{-2}$
20 hr	$1.22 \pm 0.06 \times 10^{-2}$		20 hr	$1.02 \pm 0.06 \times 10^{-2}$
24 hr	$1.01 \pm 0.07 \times 10^{-2}$		24 hr	$8.50 \pm 0.04 \times 10^{-3}$
UV, catalyst & HP			UV & TiO_2	
Time	Conc (M)		Time	Conc (M)
Start	$1.52 \pm 0.03 \times 10^{-2}$		Start	$1.05 \pm 0.02 \times 10^{-2}$
1 hr	$1.04 \pm 0.02 \times 10^{-2}$		1 hr	$1.03 \pm 0.01 \times 10^{-2}$
4 hr	$4.41 \pm 0.09 \times 10^{-7}$		4 hr	$1.02 \pm 0.04 \times 10^{-2}$
20 hr	$< 10^{-7}$		20 hr	$9.07 \pm 0.05 \times 10^{-3}$
24 hr	$< 10^{-7}$		24 hr	$9.26 \pm 0.03 \times 10^{-3}$

Table 3.1-1: Summary of results of photocatalytic treatment of an aqueous vinyl acetic acid solution.

Calculation of percent reduction over time suggests that catalyst, in the presence of hydrogen peroxide and UV light was the most efficient means of degradation, resulting in loss of in excess of 99 %. Degradation occurred such that UV detection limits were exceeded. UV light only proved to be the next best method of compound degradation, resulting in a 29.89 ±0.01% reduction over a period of 24 hours. Use of the catalyst with UV light was the third most effective method of degrading vinyl acetic acid, with a reduction in concentration over 24 hours of 26.09 ±0.03%. The least effective method of compound degradation in this case was combining TiO_2 with UV light, to yield only 11.58 ±0.04% reduction in total concentration.

The model compound chosen to represent the resin acids is abietic acid. It can be detected by HPLC at a wavelength of 230 nm with a mobile phase of 74% water, 1% tris buffer, and 25% acetonitrile, its retention time is approximately 7 min (Figure 3.1- 2 and 3.1-3).

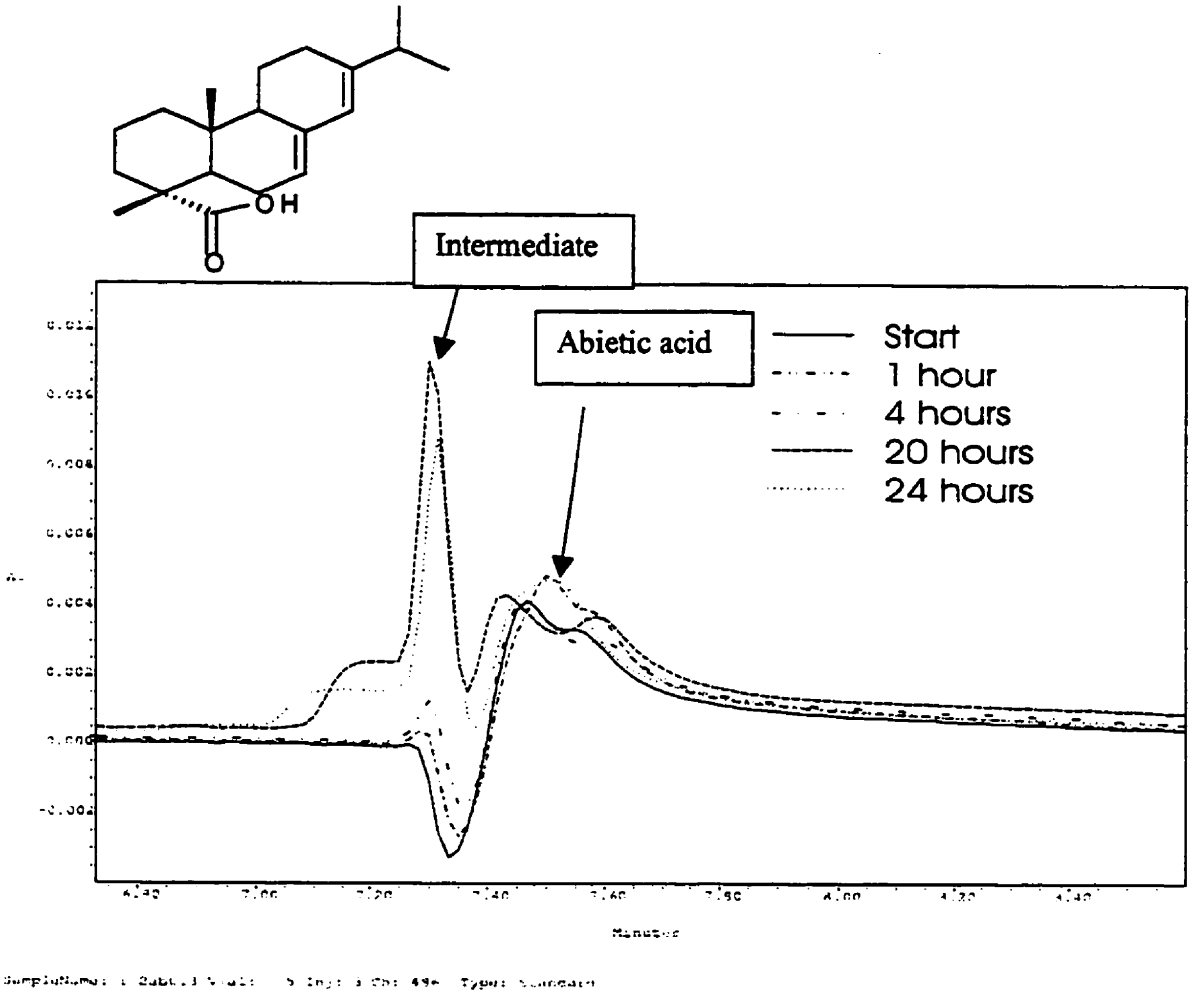

Figure 3.1-2: HPLC chromatogram for abietic acid. Treatment with supported catalyst.

The opacity of aqueous abietic acid causes a filter effect inhibiting light from reaching the catalyst during treatments; thus, inhibiting the oxidation reactions. Treatments involving the catalyst and Degussa P25 TiO_2 were started with an initial 24 hour period of direct photolysis.

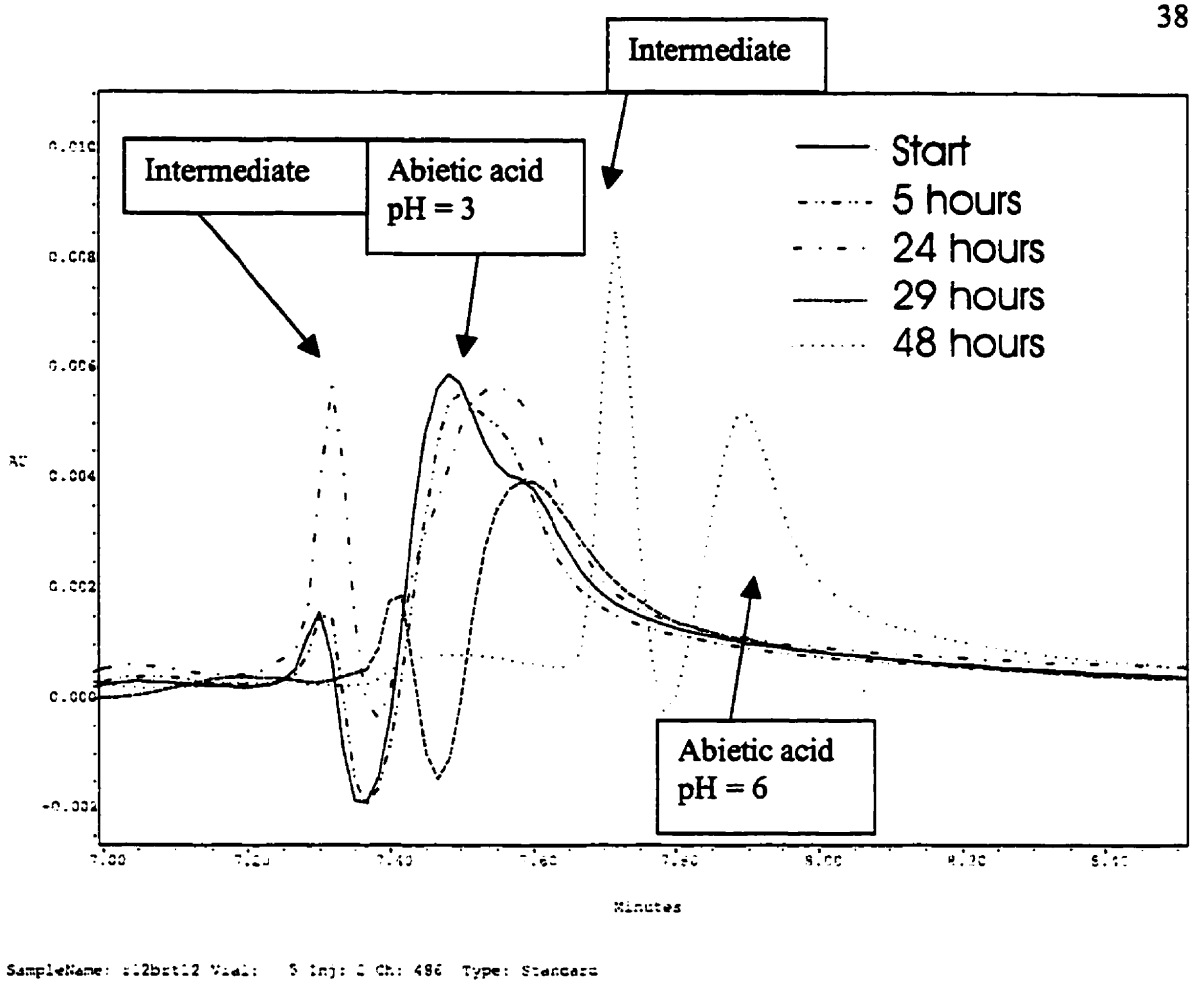

Figure 3.1-3: HPLC chromatogram of abietic acid treatment with supported catalyst with initial 24 hour period of direct photolysis.

In Figure 3.1-3 we can see that there is a major shift in retention time for abietic acid and its intermediates when the abietic acid is treated with direct photolysis for 24 hours followed by catalyst or catalyst and hydrogen peroxide. This change in retention time is related to a pH change from pH = 3 to pH = 6. This might be due to ion interaction between the abietic acid and the column when the pH is higher.

Correlating the peak area to a calibration curve suggests that the different methods of treatment have yielded the results outlined in Table 3.1-2. Abietic acid is problematic for treatment because it forms a colloidal suspension in water

thereby forming a UV filter inhibiting light from reaching the catalyst. Thus, an initial 24 hour direct photolysis treatment was done before treatment with catalyst and catalyst and hydrogen peroxide. However, we notice that the addition of hydrogen peroxide only helps in the initial stages of degradation but not in the overall degradation. It was seen earlier in section 1.2 that hydrogen peroxide helps in initiating the organic compound oxidation, gets used up and; therefore, is inactive for the remainder of the treatment period. Further additions of hydrogen peroxide, however, were not effective. Hydrogen peroxide appears to function as an initiator.

UV only		UV & catalyst	
Time	Conc (M)	Time	Conc (M)
Start	$2.36 \pm 0.03 \times 10^{-3}$	Start	$2.07 \pm 0.09 \times 10^{-3}$
1 hr	$2.23 \pm 0.09 \times 10^{-3}$	1 hr	$1.98 \pm 0.01 \times 10^{-3}$
4 hr	$1.95 \pm 0.08 \times 10^{-3}$	4 hr	$2.09 \pm 0.07 \times 10^{-3}$
20 hr	$1.69 \pm 0.01 \times 10^{-3}$	20 hr	$1.87 \pm 0.01 \times 10^{-3}$
24 hr	$1.78 \pm 0.02 \times 10^{-3}$	24 hr	$1.68 \pm 0.05 \times 10^{-3}$
UV, catalyst & HP		UV & TiO_2	
Time	Conc (M)	Time	Conc (M)
Start	$2.40 \pm 0.05 \times 10^{-3}$	Start	$2.23 \pm 0.02 \times 10^{-3}$
1 hr	$2.15 \pm 0.07 \times 10^{-3}$	1 hr	$2.11 \pm 0.09 \times 10^{-3}$
4 hr	$1.79 \pm 0.01 \times 10^{-3}$	4 hr	$1.95 \pm 0.09 \times 10^{-3}$
20 hr	$1.32 \pm 0.02 \times 10^{-3}$	20 hr	$1.69 \pm 0.04 \times 10^{-3}$
24 hr	$1.33 \pm 0.05 \times 10^{-3}$	24 hr	$1.89 \pm 0.02 \times 10^{-3}$

Degradation Following 24 hours Preliminary Direct Photolysis

UV only		UV & catalyst	
Time	Conc (M)	Time	Conc (M)
Start	$2.36 \pm 0.03 \times 10^{-3}$	Start	$2.12 \pm 0.02 \times 10^{-3}$
1 hr	$2.23 \pm 0.09 \times 10^{-3}$	5 hr	$1.63 \pm 0.02 \times 10^{-3}$
4 hr	$1.95 \pm 0.08 \times 10^{-3}$	24 hr	$1.56 \pm 0.02 \times 10^{-3}$
20 hr	$1.69 \pm 0.01 \times 10^{-3}$	29 hr	$1.45 \pm 0.01 \times 10^{-3}$
24 hr	$1.78 \pm 0.02 \times 10^{-3}$	48 hr	$8.53 \pm 0.02 \times 10^{-4}$
UV, catalyst & HP		UV & TiO_2	
Time	Conc (M)	Time	Conc (M)
Start	$2.34 \pm 0.08 \times 10^{-3}$	Start	$2.19 \pm 0.02 \times 10^{-3}$
5 hr	$1.91 \pm 0.03 \times 10^{-3}$	5 hr	$2.13 \pm 0.09 \times 10^{-3}$
24 hr	$1.56 \pm 0.06 \times 10^{-3}$	24 hr	$1.92 \pm 0.03 \times 10^{-3}$
29 hr	$1.56 \pm 0.06 \times 10^{-3}$	29 hr	$1.76 \pm 0.01 \times 10^{-3}$
48 hr	$1.45 \pm 0.02 \times 10^{-3}$	48 hr	$1.72 \pm 0.02 \times 10^{-3}$

Table 3.1.2: Summary of results of photocatalytic treatment of an aqueous abietic acid solution.

As previously mentioned, formation of a colloidal suspension necessitated 24 hours of direct photolysis when using catalyst before catalyst addition. In order to effectively compare results, this was also undertaken for the runs that incorporated only UV light and those that used TiO_2. For samples where no irradiation took place, it can be observed that the UV light only resulted in 24.64 ±0.01percent reduction. This is a comparably greater reduction than those runs which used the catalyst with UV light or TiO_2 with UV light without the direct photolysis, giving percent reductions of 19.12 ±0.01% and 14.93 ±0.06% respectively. As expected, however, the addition of hydrogen peroxide greatly increased the efficiency for the reaction, resulting in overall reduction of 44.65 ±0.03%. In the reactions where 24 hours of photolysis occurred before addition of

the catalyst, the observed percent reduction was increased substantially for UV light with the catalyst from 19.12 ±0.02% to 59.81 ±0.04%. The hydrogen peroxide appears to be slightly less efficient in this case, resulting in a percent reduction of only 38.02 ±0.03% in contrast to the 44.65 ±0.02% observed without preliminary photolysis. In addition to this, the UV light with titania resulted in a percent reduction of 21.60 ±0.01%, slightly increased from the run without preliminary direct photolysis.

3.2 Sterol Esters

As mentioned in chapter 2 the model compound chosen to represent the sterol esters is ethylnonanoate. It can be detected by HPLC at a wavelength of 240 nm with a mobile phase of 24% water, 1% tris buffer, and 75% acetonitrile, its retention time is approximately 20 min (Figure 3.2-1).

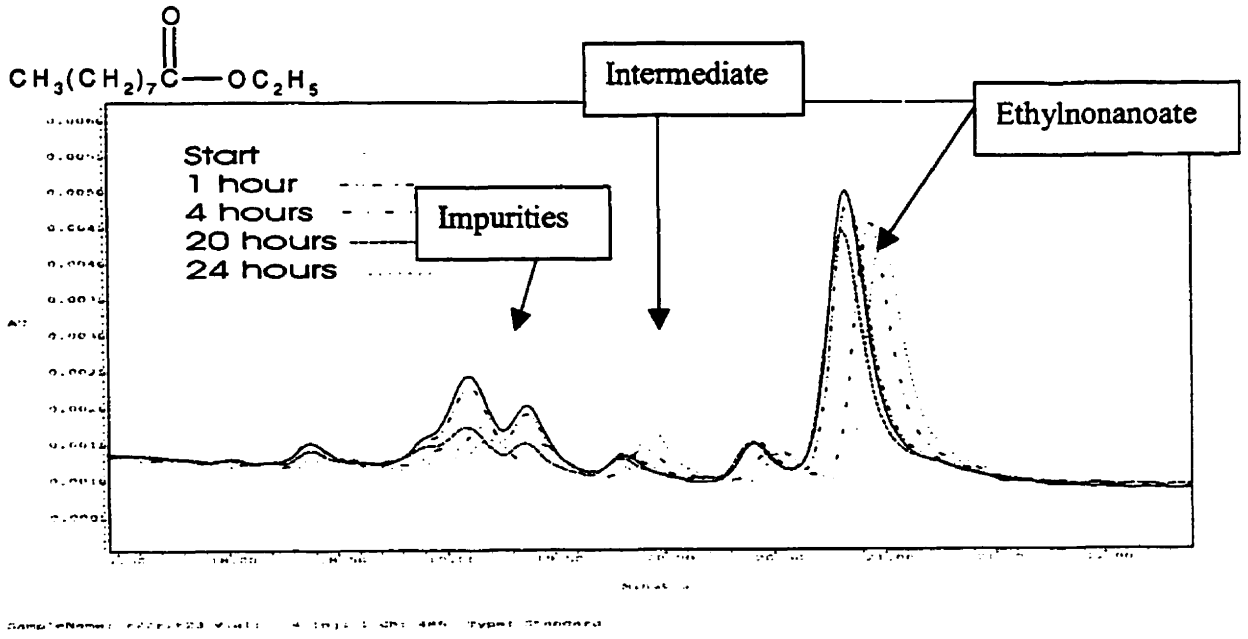

Figure 3.2-1: HPLC chromatogram for the treatment of ethylnonanoate with the supported catalyst.

A new peak can be seen forming at shorter retention time than the ethylnonanoate peak.

Correlating the peak area to a calibration curve suggests that the different methods of treatment have yielded the results outlined in Table 3.2-1. The lack of chromophores makes it virtually impossible to treat ethylnonanote by direct photolysis; thus the catalyst is needed in this case. It is again seen that the addition of hydrogen peroxide to the catalyst helps initiate the oxidation of the compound. However, the degussa P25 TiO_2 is less effective than the supported catalyst. This substrate is more hydrophobic.

UV only	
Time	Conc (M)
Start	$2.66 \pm 0.02 \times 10^{-2}$
1 hr	$2.19 \pm 0.02 \times 10^{-2}$
4 hr	$1.49 \pm 0.07 \times 10^{-2}$
20 hr	$2.03 \pm 0.05 \times 10^{-2}$
24 hr	$1.93 \pm 0.01 \times 10^{-2}$

UV & catalyst	
Time	Conc (M)
Start	$2.14 \pm 0.04 \times 10^{-2}$
1 hr	$2.42 \pm \times 0.03\ 10^{-2}$
4 hr	$2.30 \pm \times 0.01\ 10^{-2}$
20 hr	$1.15 \pm \times 0.01\ 10^{-2}$
24 hr	$8.40 \pm \times 0.05\ 10^{-3}$

UV, catalyst & HP	
Time	Conc (M)
Start	$2.73 \pm 0.03 \times 10^{-2}$
1 hr	$2.34 \pm \times 0.07\ 10^{-2}$
4 hr	$1.90 \pm \times 0.07\ 10^{-2}$
20 hr	$7.52 \pm \times 0.02\ 10^{-3}$
24 hr	$4.58 \pm \times 0.05\ 10^{-3}$

UV & TiO_2	
Time	Conc (M)
Start	$2.47 \pm 0.01 \times 10^{-2}$
1 hr	$2.28 \pm \times 0.05\ 10^{-2}$
4 hr	$2.09 \pm \times 0.02\ 10^{-2}$
20 hr	$1.17 \pm \times 0.02\ 10^{-2}$
24 hr	$1.30 \pm \times 0.02\ 10^{-2}$

Table 3.2-1: Summary of results of photocatalytic treatment of an aqueous solution of ethylnonanoate

Percent reduction of ethyl nonanoate was most efficient using catalyst with hydrogen peroxide coupled with light irradiation. This resulted in 83.23 ±0.03% reduction. The catalyst with UV light shows the next highest percent reduction with 61.83 ±0.08% reduction observed over the period of 24 hours. Following this, UV

light with titania gave percent reduction of 47.16 ±0.06% and UV light only resulted in 27.27 ±0.06% reduction.

3.3 Triglycerides

As mentioned in chapter 2 the model compound chosen to represent the triglycerides is triacetin. It can be detected by HPLC at a wavelength of 240 nm with a mobile phase of 24% water, 1% tris buffer, and 75% acetonitrile, its retention time is approximately 8 min (Figure 3.3-1).

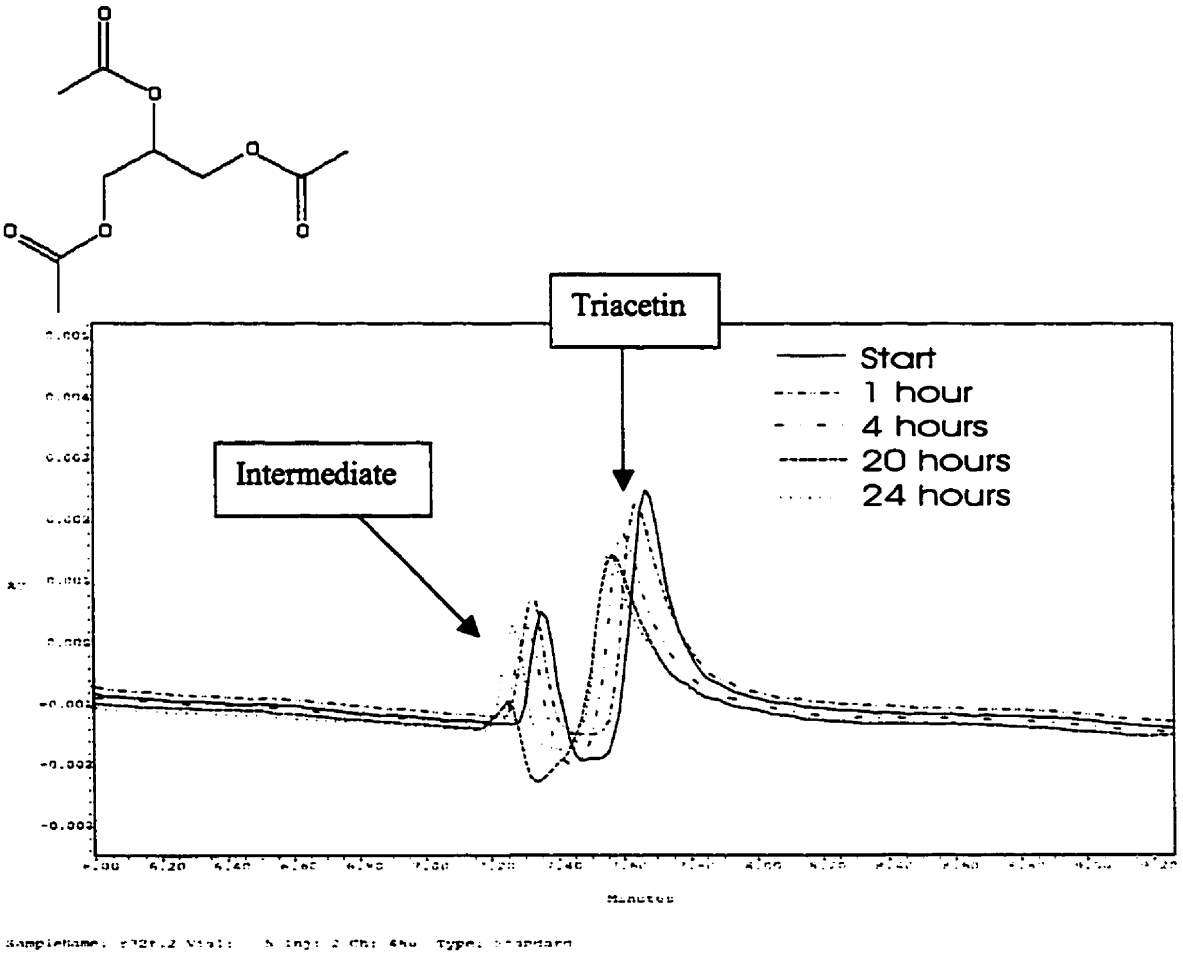

Figure 3.3-1: HPLC chromatogram for the treatment of triacetin with the supported catalyst.

Correlating the peak area to a calibration curve suggests that the different methods of treatment have yielded the results outlined in Table 3.3-1. Again, the lack of chromophores makes it virtually impossible to treat triacitin by direct photolysis; thus the catalyst is needed in this case and is effective in absorbing the triacitin molecule to its surface for the oxidation of triacitin. It is again seen that the addition of hydrogen peroxide to the catalyst helps initiate the oxidation of the compound. However, the degussa P25 TiO_2 is less effective than the supported catalyst.

UV only		UV & catalyst	
Time	Conc (M)	Time	Conc (M)
Start	$4.48 \pm 0.09 \times 10^{-2}$	Start	$4.75 \pm 0.08 \times 10^{-2}$
1 hr	$4.28 \pm 0.05 \times 10^{-2}$	1 hr	$4.61 \pm 0.04 \times 10^{-2}$
4 hr	$4.20 \pm 0.06 \times 10^{-2}$	4 hr	$4.39 \pm 0.01 \times 10^{-2}$
20 hr	$4.02 \pm 0.06 \times 10^{-2}$	20 hr	$4.29 \pm 0.09 \times 10^{-2}$
24 hr	$4.05 \pm 0.09 \times 10^{-2}$	24 hr	$3.90 \pm 0.06 \times 10^{-2}$
UV, catalyst & HP		UV & TiO_2	
Time	Conc (M)	Time	Conc (M)
Start	$4.37 \pm 0.07 \times 10^{-2}$	Start	$4.50 \pm 0.03 \times 10^{-2}$
1 hr	$4.06 \pm 0.07 \times 10^{-2}$	1 hr	$4.47 \pm 0.07 \times 10^{-2}$
4 hr	$3.94 \pm 0.02 \times 10^{-2}$	4 hr	$4.31 \pm 0.04 \times 10^{-2}$
20 hr	$3.49 \pm 0.07 \times 10^{-2}$	20 hr	$4.36 \pm 0.04 \times 10^{-2}$
24 hr	$3.42 \pm 0.06 \times 10^{-2}$	24 hr	$4.17 \pm 0.05 \times 10^{-2}$

Table 3.3-1: Summary of results of photocatalytic treatment of an aqueous triacetin solution.

It was noticed that the percent reduction for this compound was relatively low in all cases. The most efficient degradation was seen to result from the

catalyst with hydrogen peroxide in the presence of UV light. This resulted in a reduction of 21.82 ±0.02%. In addition to this, UV light with the catalyst was also relatively good for this compound, resulting in a total percent reduction of 17.95 ±0.03%. Both UV light only and UV light with titania yielded poor reduction overall with only 9.67 ±0.03 and 7.25 ±0.01 percent reduction occurring respectively.

3.4 Lignins

As mentioned in chapter 2 the model compound chosen to represent the lignins is the mixture known as "lignin alkali". It can be detected by HPLC at a wavelength of 240 nm with a mobile phase of 74% water, 1% tris buffer, and 25% acetonitrile, its retention time is approximately 4 min (Figure 3.4-1). The peak due to the lignins is a broad peak spanning the 3.7 min to 4 min range because it is mixture.

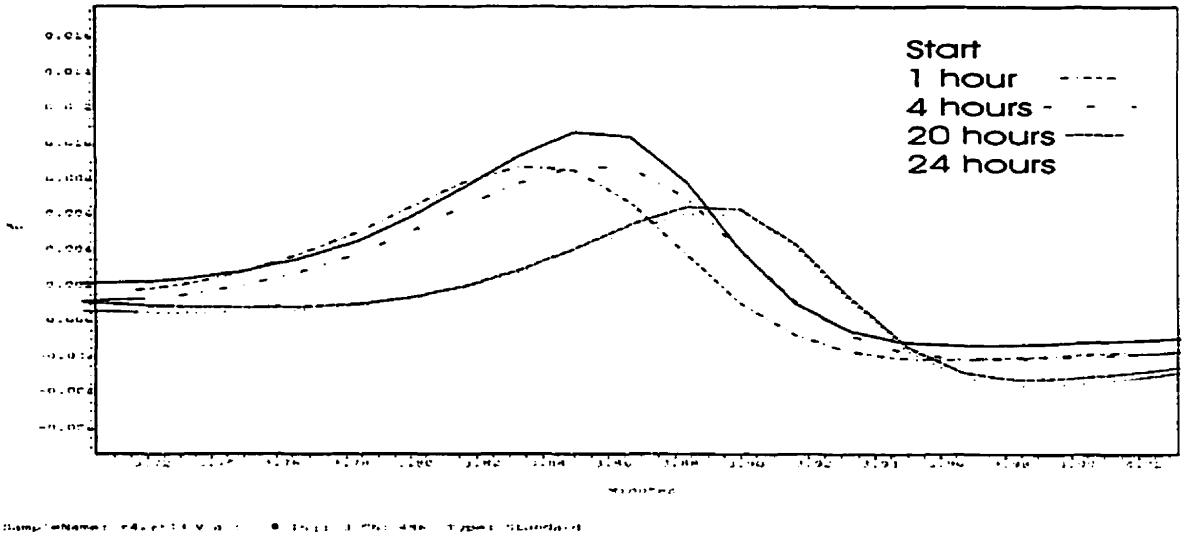

Figure 3.4-1: HPLC chromatogram of lignin treatment with the supported catalyst. The complex mixture character is evident in the broad peaks. Shift from a shorter retention time to a longer retention time is due to a change in pH from more acidic to neutral range.

Initial observation using UV-visible spectrometry indicates that our different treatments are relatively ineffective overall towards the lignin alkali, Figures 3.4-2 to 3.4-5. There is no aromatic ring opening observed; however polymeric breakdown without ring opening shows no decrease in the spectra because the signal is due to aromatic rings.

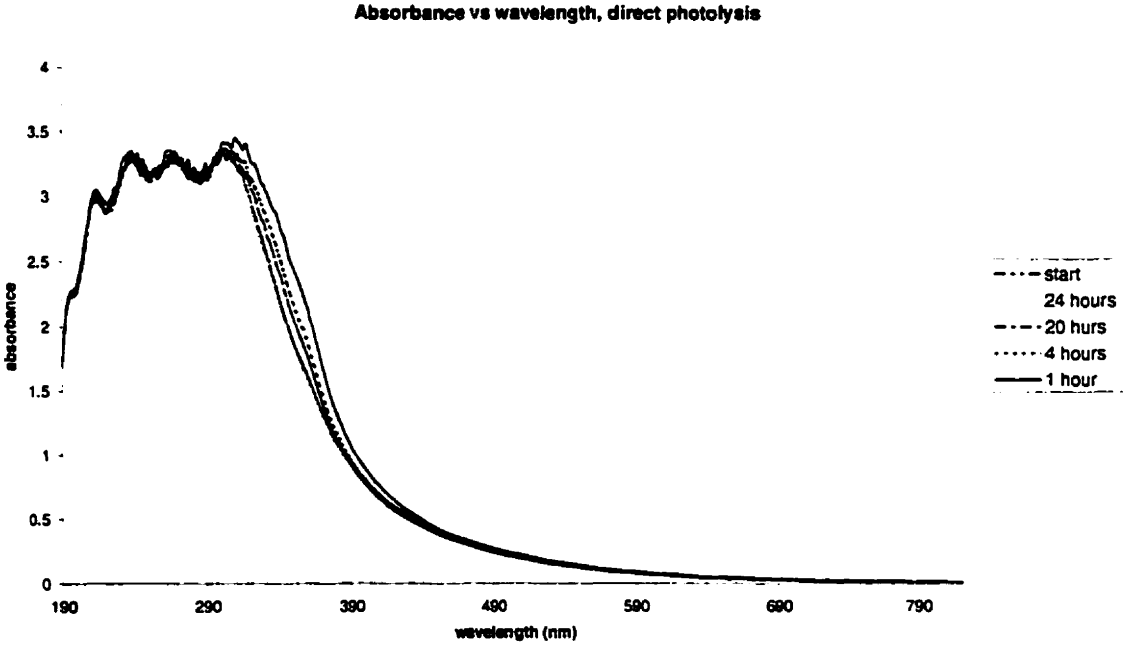

Figure 3.4-2: UV-visible spectra after direct photolysis on lignin alkali

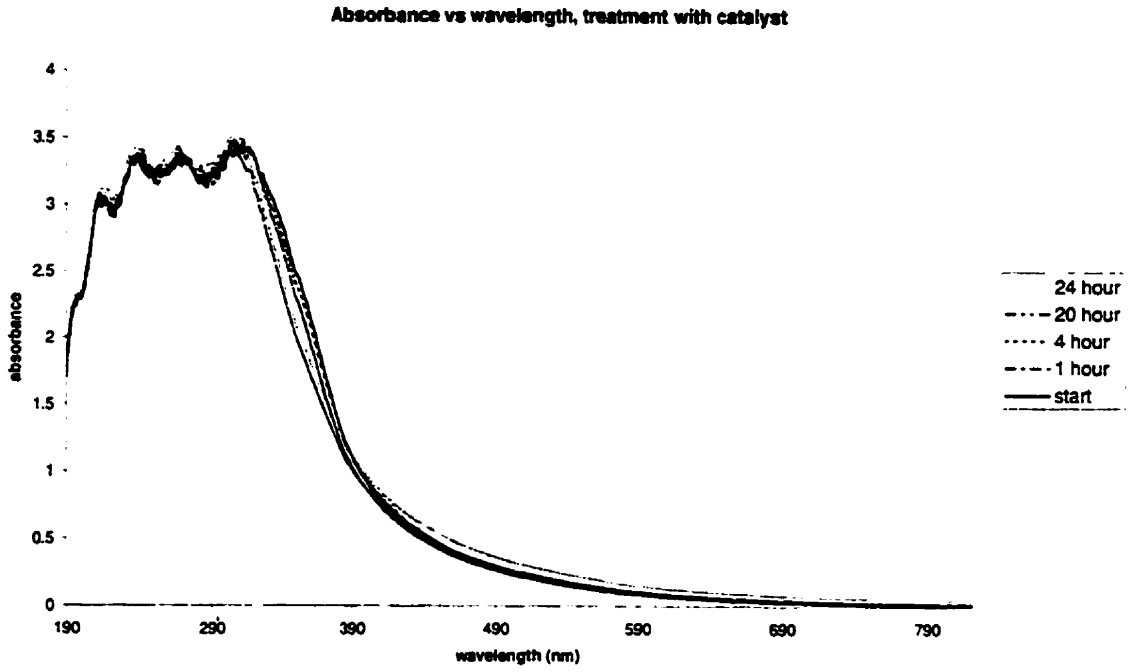

Figure 3.4-3: UV-visible spectra after lignin alkali treatment with the supported catalyst.

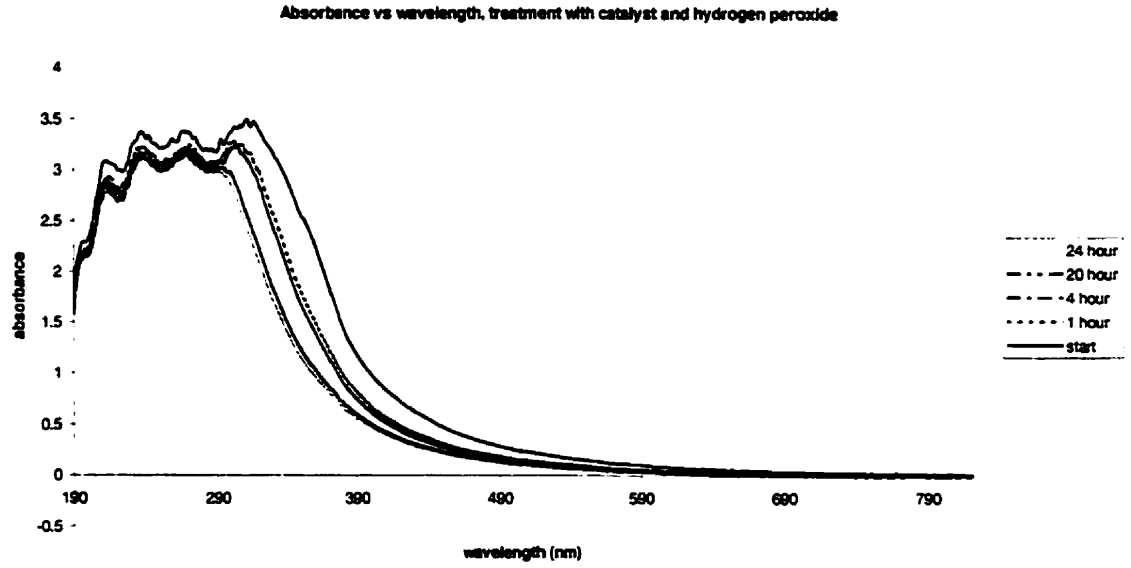

Figure 3.4-4: UV-visible spectra after lignin alkali treatment with catalyst and hydrogen peroxide

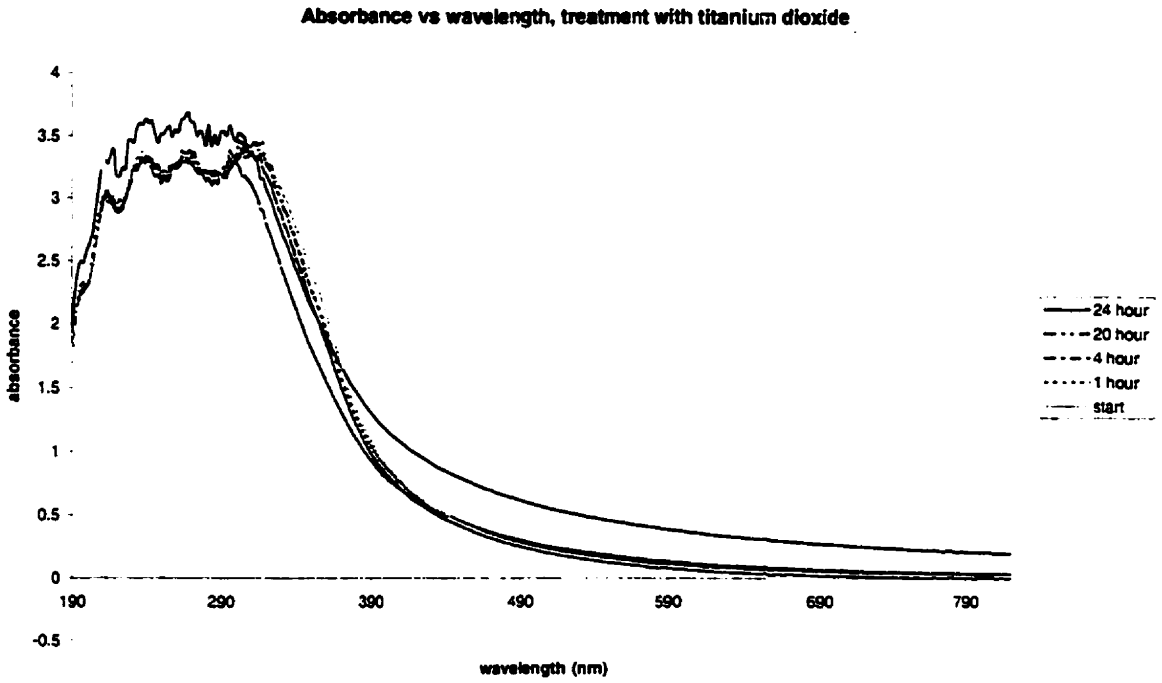

Figure 3.4-5: UV-Visible spectra after lignin alkali treatment with titanium dioxide

UV-Visible spectrometry data analysis has shown that there is bleaching at a 355 nm, which is the photolysis lamps' maximum wavelength. The n to π^* transition in ketones is populated at this wavelength. Intermediates that produce colour at wavelengths grater than 450 nm (Figure 3.4-6) are formed. Thus photocatalytic oxidation is occurring, but prior to destruction of the aromatic rings responsible for much of the UV absorbance.

Differential spectrometry was used to observe the UV spectra with increased sensitivity. The principle behind this technique is that small changes on a large scale are difficult to observe. As such, it is easier if one observes the differences between the successive spectra in order to get a better picture of what is occurring. If measurements are made relative, changes become independent of

absorptivity in the wavelength region in question. Essentially, the difference between the spectrum in question and the initial spectrum is taken and normalized

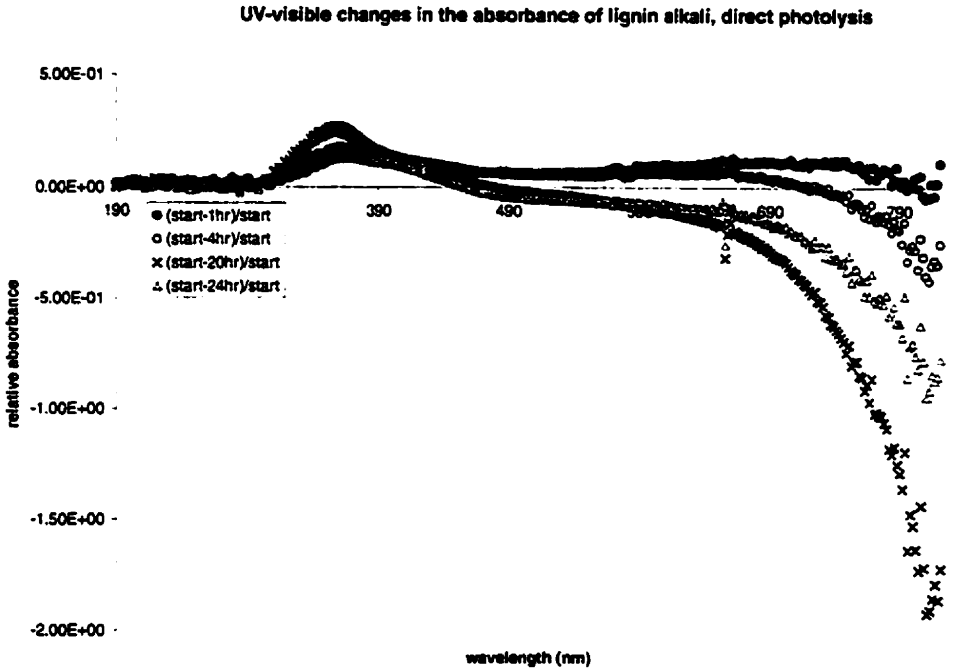

Figure 3.4-6: Differential UV-visible spectra, showing the changes occurring during direct photolysis of lignin alkali.

with respect to the starting spectrum. As a result, small differences between the spectra, otherwise unnoticeable, become much more apparent and observable.

Upon treatment with the supported catalyst there is also bleaching observed. Most importantly we see formation of the coloured intermediates followed by some degradation of these; however this is complicated by a continuing formation of these coloured intermediate compounds, (Figure 3.4-7).

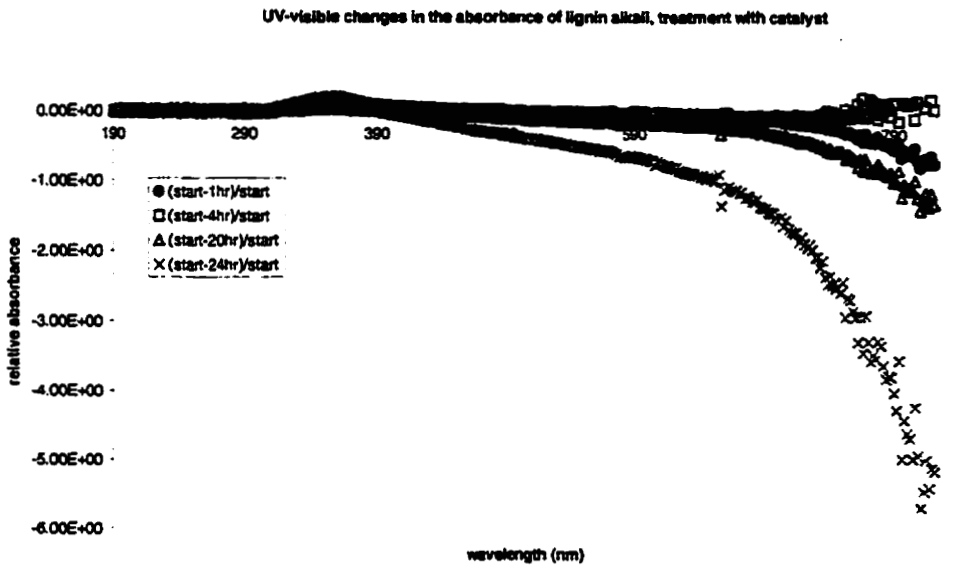

Figure 3.4-7: Differential UV-visible spectra, showing the changes occurring during photolysis of lignin alkali with the catalyst.

Upon treatment with the catalyst and hydrogen peroxide there is more important bleaching observed. Moreover there is a more important prompt degradation of the coloured intermediates and slower secondary formation of such species, (Figure 3.4-8).

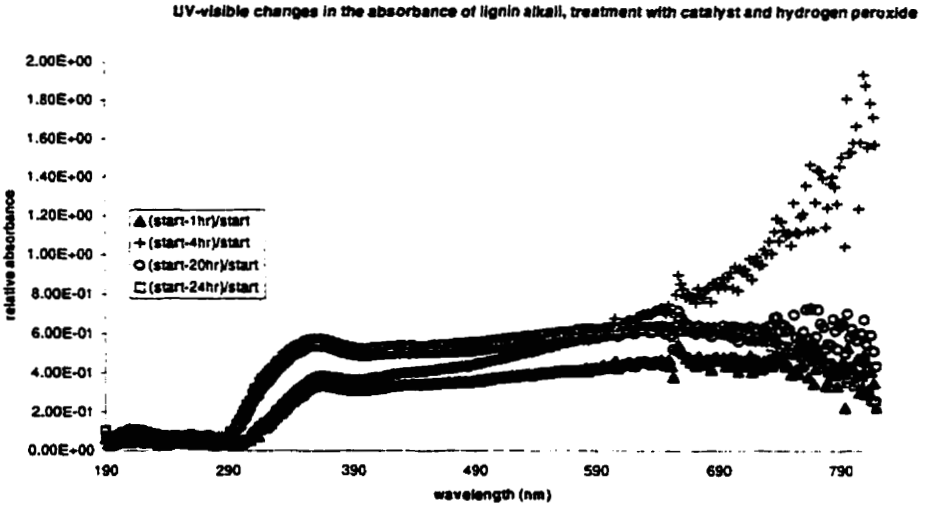

Figure 3.4-8: Differential UV-visible spectra, showing the changes occurring during photolysis of lignin alkali with the catalyst and hydrogen peroxide.

Treatment with titanium dioxide yields results similar to those from the treatment with the supported catalyst, but with smaller changes. There is less bleaching observed and not as much coloured intermediate formation, (Figure 3.4-9).

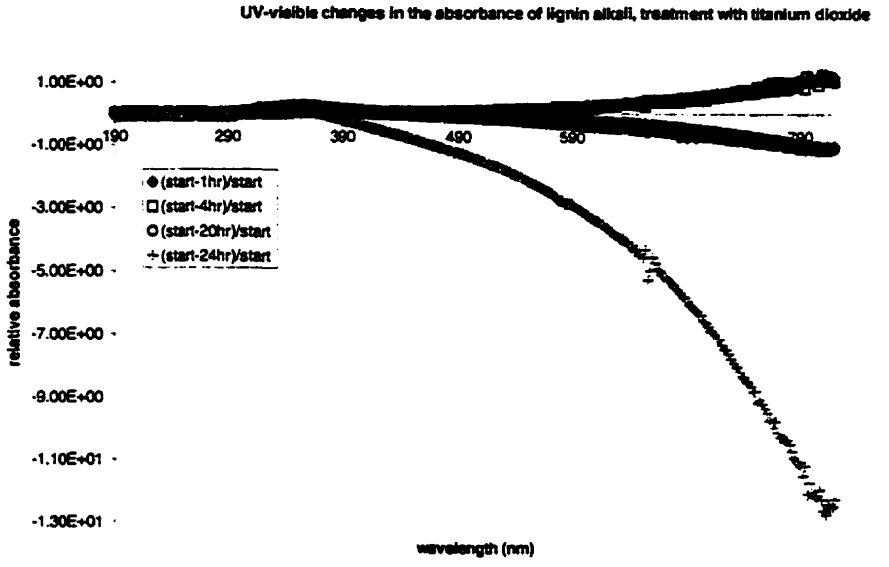

Figure 3.4-9: Differential UV-visible spectra, showing the changes occurring during photolysis of lignin alkali with titanium dioxide

Decrease of peak area in the 3.7 min to 4 min range indicated that the different methods of treatment have yielded the results outlined in table 3.4-1. There is not a large decrease in the overall amount of lignin related compounds present because lignins are very large, polymeric molecules, see Figure 1.3.2-2. In this period, breakdown of polymers is the main reaction and aromatic ring opening is not yet important.

Lignin Alkali			
UV only		UV & catalyst	
Time	Conc (ppm)	Time	Conc (ppm)
Start	584.12±0.08	Start	584.75±0.03
1 hr	577.23±0.01	1 hr	572.28±0.04
4 hr	573.47±0.04	4 hr	566.09±0.08
20 hr	566.11±0.05	20 hr	558.75±0.02
24 hr	562.86±0.06	24 hr	557.04±0.04
UV, catalyst & HP		UV & TiO_2	
Time	Conc (ppm)	Time	Conc (ppm)
Start	583.24±0.03	Start	582.12±0.07
1 hr	569.56±0.04	1 hr	574.86±0.07
4 hr	562.64±0.04	4 hr	568.96±0.01
20 hr	542.40±0.01	20 hr	562.32±0.01
24 hr	538.52±0.01	24 hr	559.97±0.01

Table 3.4-1: Summary of results of photocatalytic treatment of an aqueous solution of lignin alkali.

The most effective reduction observed occurred using the catalyst in the presence of hydrogen peroxide and UV light. This resulted in only an 7.66 ±0.02% reduction overall in UV absorbing species. Degradation by directphotolysis, photolysis with the catalyst, and photolysis with titania were equally effective in degradation of the UV absorbing species; they resulted in 3.63 ± 0.04, 4.73 ± 0.05, and 3.80 ± 0.04 percent reduction respectively.

3.5 Model Whitewater

The model water is a "model" of a highly recycled whitewater, from Howe Sound Pulp and Paper Mill, called "model" highly recycled whitewater. It was furnished by the UBC group of Prof. J.N. Saddler. It was prepared from fresh Spruce-Pine-Fir chips obtained from Canadian Forest Product Ltd. Thermomechanical pulp was made from these chips at PAPRICAN's pilot plant using a Sunds Defibrator TMP 300 single disk laboratory refiner. The model whitewater was prepared by washing the thermomechanical pulp with distilled water in a batch process. Each batch contained 3.6 kg of pulp washed with 180 L of distilled water at 60°C for 20 min with stirring. The pulp suspension was dewatered using a screw press to an approximate consistency of 45%, the collected water was the initial whitewater. In order to model a recycled whitewater; the collected whitewater was then used to wash a new batch of thermomechanical pulp. The model water was used for washes five times then collected and called highly recycled whitewater.

Four 100 mL portions of the model water were each treated by one of the following four methods: direct photolysis, photolysis with the UCPG204 catalyst, photolysis with the catalyst and 0.5% of hydrogen peroxide, and finally with degussa P25 TiO_2. As stated in chapter two a 10 mL portion was taken at a specific point in time. These portions were extracted with three 10mL portions of MTBE. The aqueous portion was saved for lignin analysis, which are not extracted from water by MTBE. The organic portion contains the fatty acids, resin acids,

sterol esters, and triglycerides. There was only one run of each treatment done because there was an insufficient amount of the model water to do more than one run.

The peaks of each class in the resulting chromatogram were assigned to the chosen model compound for that class. Therefore, the fatty acids were assigned to vinyl acetic acid, the resin acids were assigned to abietic acid, the sterol esters were assigned to ethylnonanoate, and finally the triglycerides were assigned to triacetin. The classes were identified by their retention time from the HPLC chromatograms of each individual model compound.

The concentrations' of the compound classes are given in terms of the model compound for each class. For example, the concentration of fatty acids at the start of treatment by direct photolysis is equivalent to 3.15 x 10^{-3} M of vinyl acetic acid. This concentration is calculated from a calibration curve of vinyl acetic acid. Each compound class is treated in the same manner.

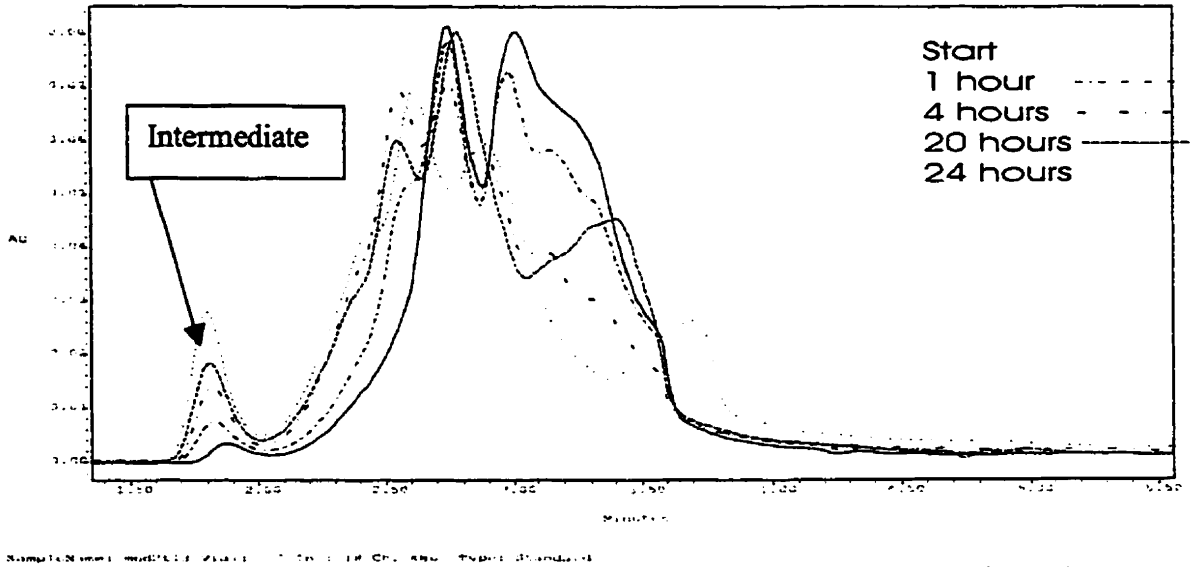

Figure 3.5-1: HPLC chromatogram of the extracted aqueous portion of model water treatment with the supported catalyst. This portion contains the lignins. Overlapping peaks were averaged, as they are all part of the lignins.

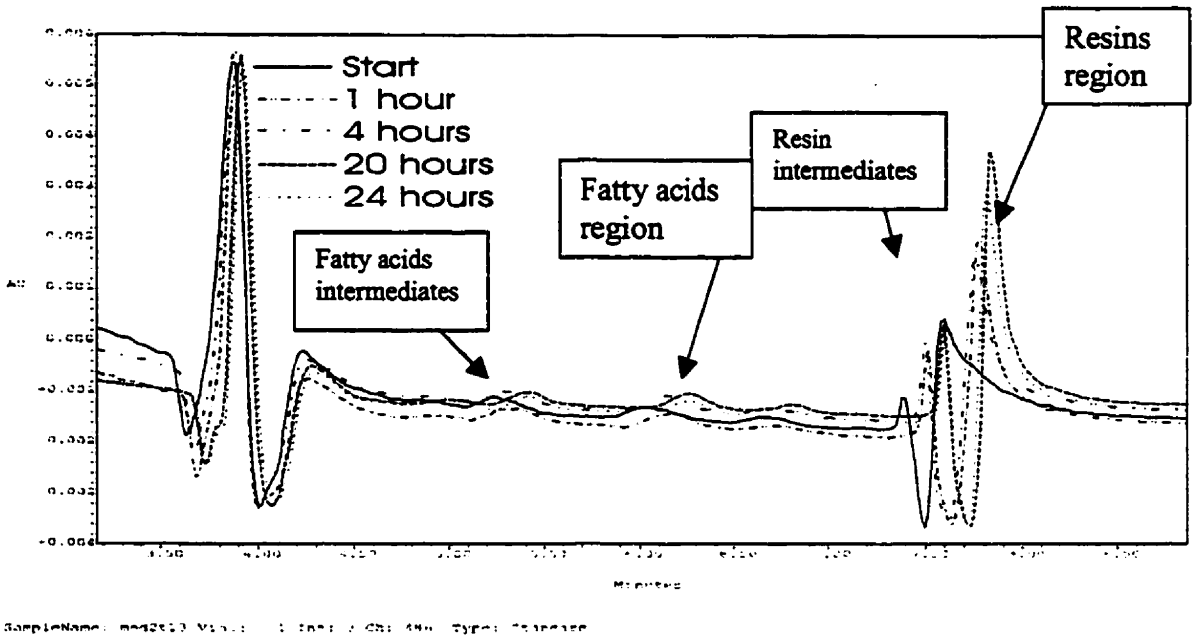

a)

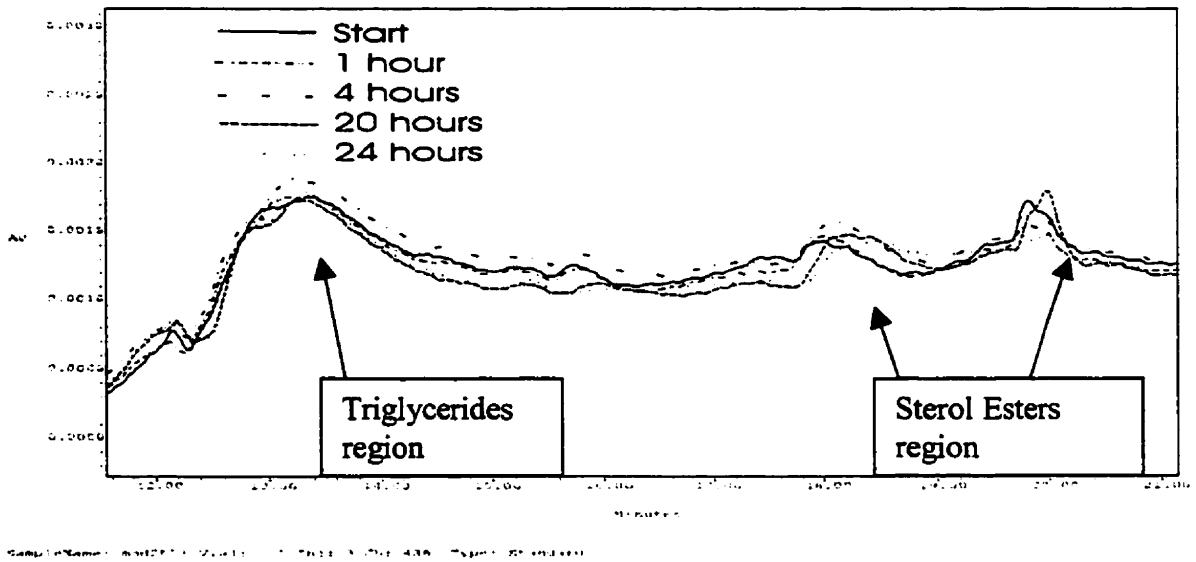

b)

Figure 3.5-2: HPLC chromatogram of the organic extract of the model water treatment with the supported catalyst. This portion contains the fatty acids and resin acids, triglycerides, and sterol esters.

As previously mentioned, the peak area was correlated with a calibration curve to obtain the concentration of the compounds. However, in this case the

class of components were correlated with the model compound chosen to represent the class.

On treatment, UV-visible spectrometry of the aqueous portion of the extracted model water, which contains the lignins, shows some change, but very little. As such, the data analysis was performed using differential UV-visible spectrometry on the lignin alkali, Figures 3.5-3 to 3.5-6.

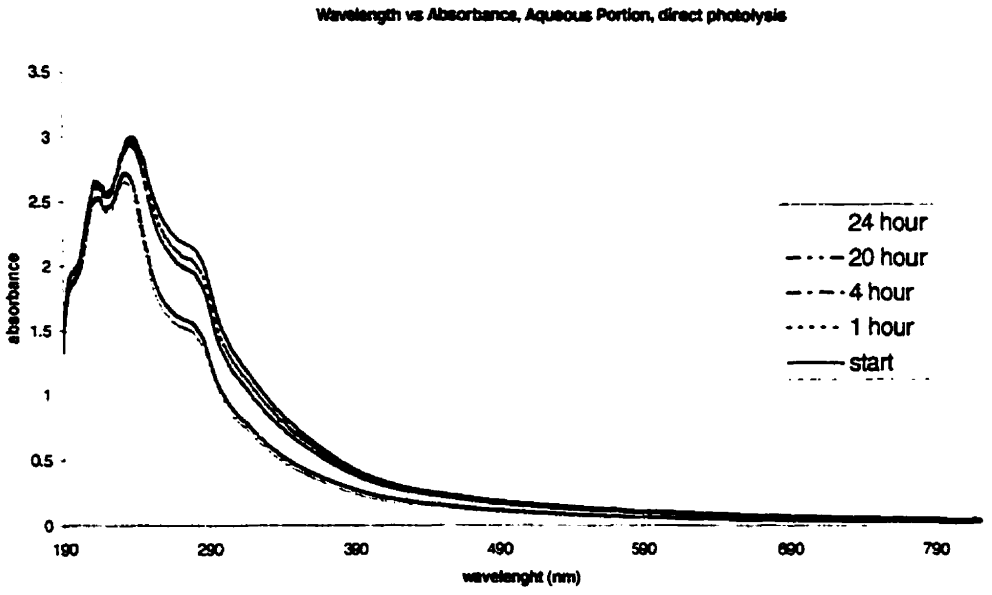

Figure 3.5-3:UV-Visible spectra after direct photolysis on the aqueous portion of model water

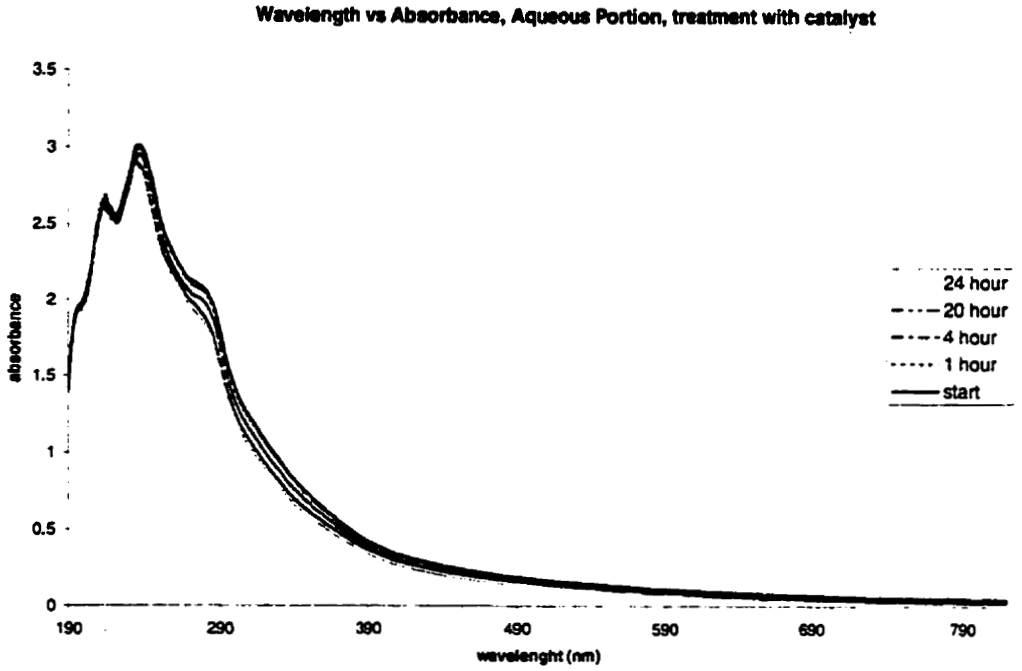

Figure 3.5-4:UV-Visible spectra after treatment with the catalyst on the aqueous portion of model water

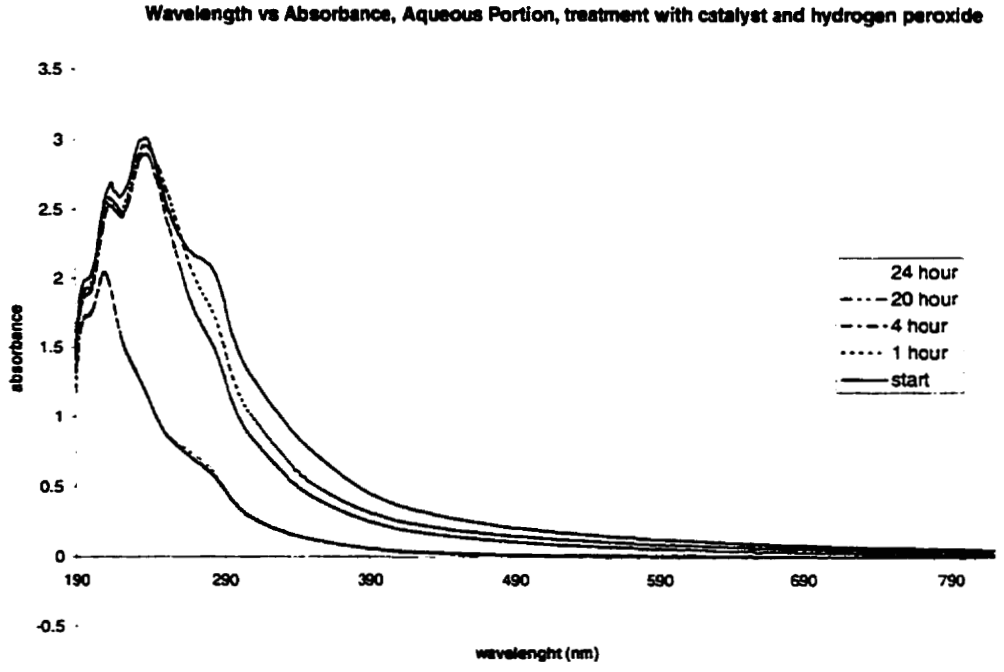

Figure 3.5-5:UV-Visible spectra after treatment with the catalyst and hydrogen peroxide on the aqueous portion of model water

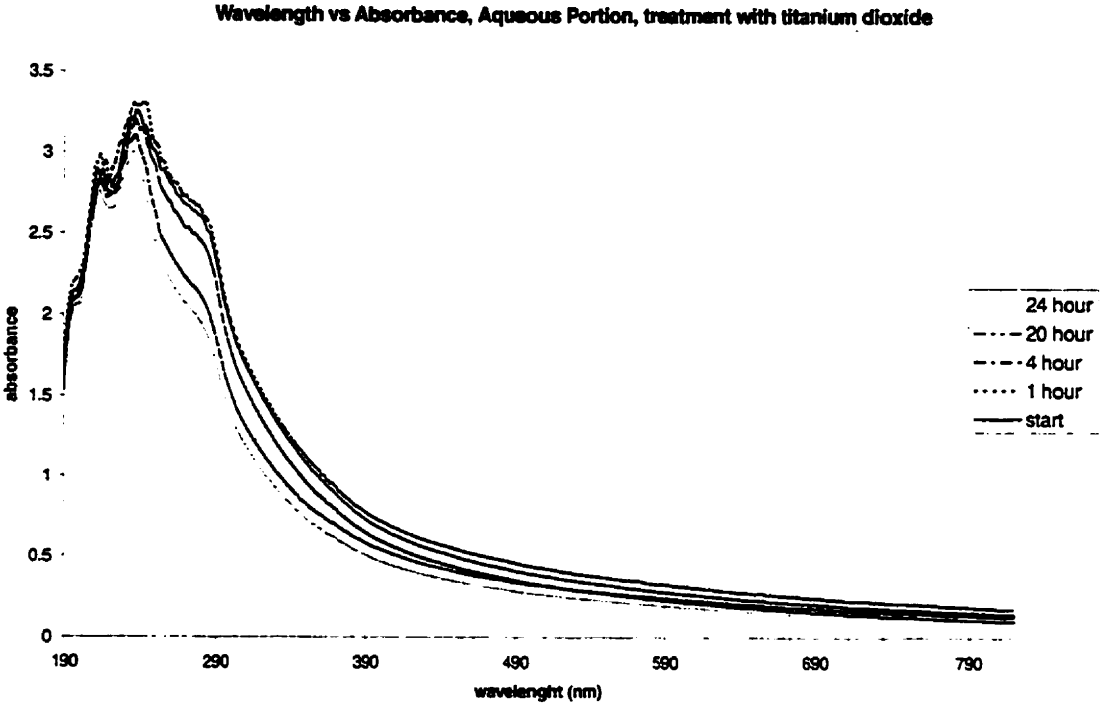

Figure 3.5-6:UV-Visible spectra after treatment with titanium dioxide on the aqueous portion of model water

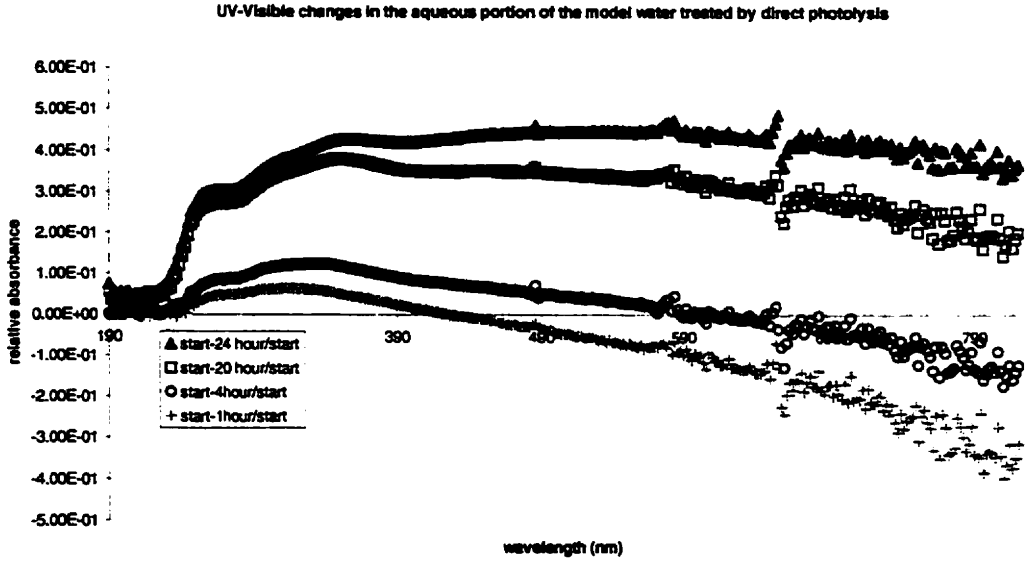

Figure 3.5-7: Differential UV-visible spectra, showing the changes occurring during direct photolysis of the aqueous portion the model water.

UV-Visible spectrometry analysis on the aqueous portion of the extracted sample shows that there is bleaching at approximately 350 nm and formation of coloured intermediates at 600 nm with treatment by direct photolysis, (Figure 3.5-7).

Treatment with the supported catalyst shows a more rapid formation of coloured intermediates followed by a reduction of these intermediates, (Figure 3.5-8).

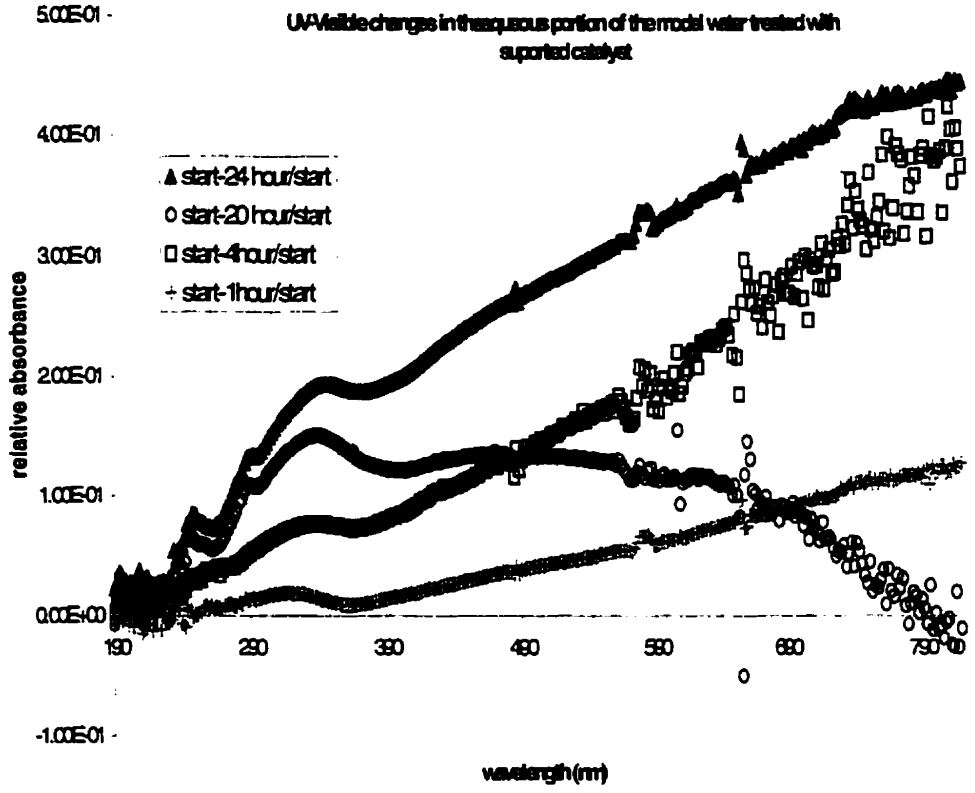

Figure 3.5-8: Differential UV-visible spectra, showing the changes occurring during photolysis of the aqueous portion the model water with the supported catalyst.

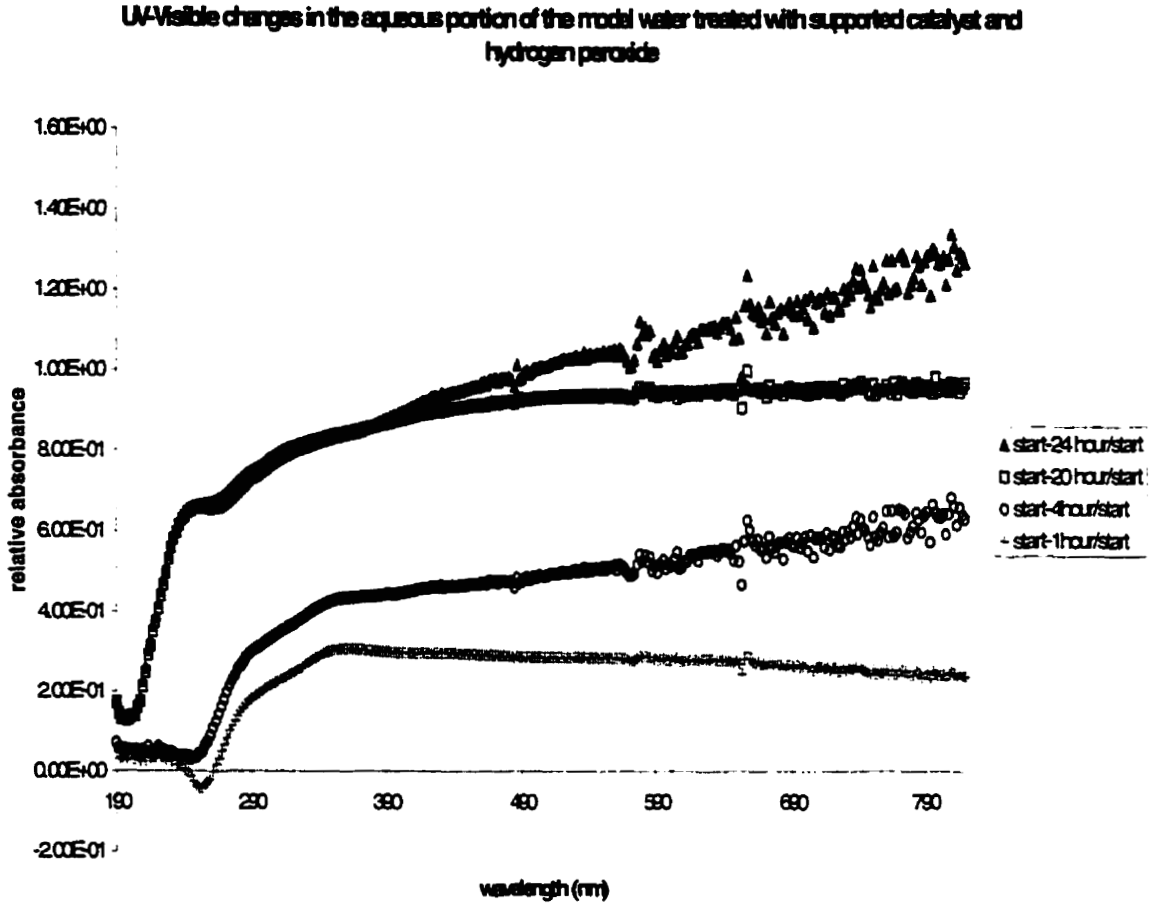

Figure 3.5-9: Differential UV-visible spectra, showing the changes occurring during photolysis of the aqueous portion of the model water with the supported catalyst and hydrogen peroxide.

Addition of hydrogen peroxide shows an almost instantaneous formation of coloured intermediates followed by a gradual degradation of the intermediates, (Figure 3.5-9).

Treatment with the degussa P25 TiO_2 shows a more rapid formation of coloured intermediates followed by a reduction of these intermediates than with treatment by direct photolysis, Figure 3.5-10.

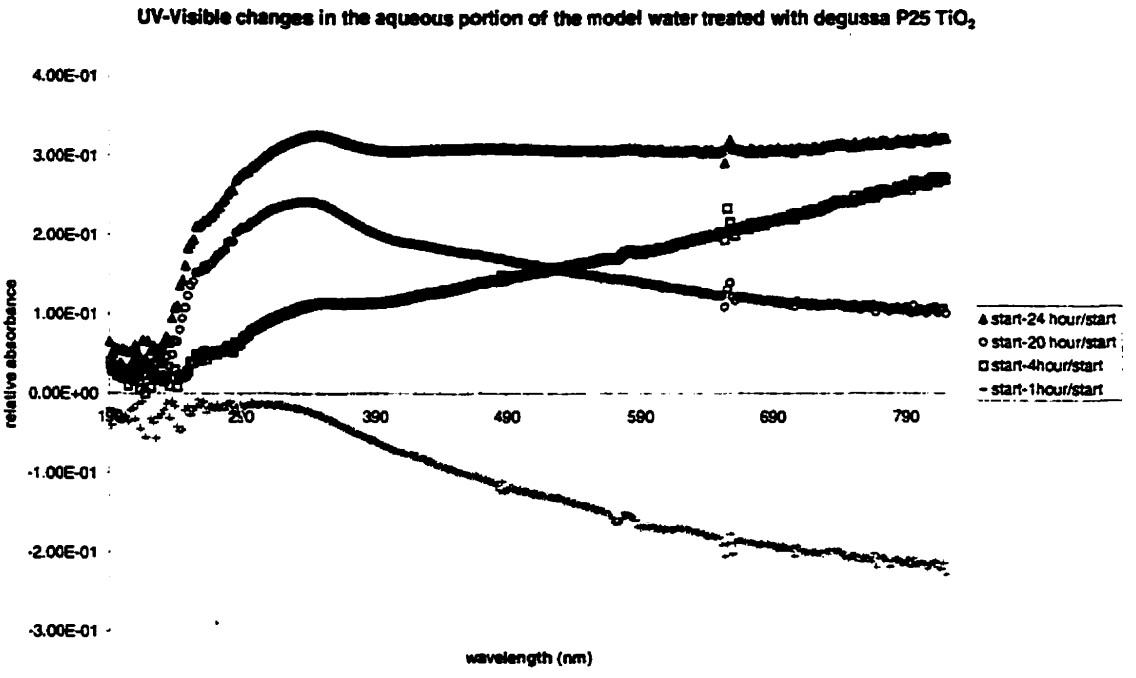

Figure 3.5-10: Differential UV-visible spectra, showing changes occurring during photolysis of the aqueous portion of the model water with titanium dioxide.

As seen in Table 3.5-1, both compound degradation and compound formation occurred in the photocatalytic treatment of the whitewater. For fatty acids, little or no degradation occurred in all cases except upon addition of hydrogen peroxide, which actually facilitated fatty acid formation. With UV light and UV light with catalyst, percent reduction was 3.15 % and 3.42 % reduction respectively. With titania, reduction was only 1.56 %. With catalyst and hydrogen peroxide in the presence of UV light, an increase of 3.65 % in fatty acids occurred. With resin acids, UV light facilitated product formation, resulting in an increase in concentration of 17.20 %. With UV light and catalyst, reduction was relatively low, resulting in consumption of only 5.4 %. Both UV light with catalyst and hydrogen peroxide and UV light with titania proved to be beneficial in this scenario, resulting

in reductions of 31.18 % and 24.87 % respectively. Triglycerides, the third class of compounds studied here, resulted in reduction in all four scenarios. In this case, UV light alone proved the most effective method of degrading the compound in question, resulting in total degradation over 24 hours as 15.10 %. UV light with catalyst also proved relatively efficient, resulting in percent degradation of 14.14 %. Both UV with TiO_2 and UV light with catalyst and peroxide were relatively inefficient in this scenario, resulting in 5.30 % and 1.28 % reduction respectively.

Fatty Acids			
UV only		UV & catalyst	
Time	Conc (M)	Time	Conc (M)
Start	3.15×10^{-3}	Start	3.06×10^{-3}
1 hr	3.01×10^{-3}	1 hr	3.34×10^{-3}
4 hr	3.02×10^{-3}	4 hr	3.25×10^{-3}
20 hr	3.04×10^{-3}	20 hr	3.12×10^{-3}
24 hr	3.05×10^{-3}	24 hr	2.95×10^{-3}
UV, catalyst & HP		UV & TiO_2	
Time	Conc (M)	Time	Conc (M)
Start	3.04×10^{-3}	Start	3.09×10^{-3}
1 hr	3.19×10^{-3}	1 hr	3.11×10^{-3}
4 hr	3.12×10^{-3}	4 hr	3.07×10^{-3}
20 hr	3.06×10^{-3}	20 hr	3.03×10^{-3}
24 hr	3.15×10^{-3}	24 hr	3.04×10^{-3}
Resin Acids			
UV only		UV & catalyst	
Time	Conc (M)	Time	Conc (M)
Start	7.15×10^{-4}	Start	1.46×10^{-3}
1 hr	3.75×10^{-4}	1 hr	1.52×10^{-3}
4 hr	7.21×10^{-4}	4 hr	1.43×10^{-3}
20 hr	8.53×10^{-4}	20 hr	1.40×10^{-3}
24 hr	8.38×10^{-4}	24 hr	1.38×10^{-3}

UV, catalyst & HP		UV & TiO_2	
Time	Conc (M)	Time	Conc (M)
Start	1.02×10^{-3}	Start	1.05×10^{-3}
1 hr	8.59×10^{-4}	1 hr	1.31×10^{-3}
4 hr	9.00×10^{-4}	4 hr	1.44×10^{-3}
20 hr	9.33×10^{-4}	20 hr	9.33×10^{-3}
24 hr	7.02×10^{-4}	24 hr	7.89×10^{-3}
Triglycerides			
UV only		UV & catalyst	
Time	Conc (M)	Time	Conc (M)
Start	3.12×10^{-2}	Start	7.15×10^{-2}
1 hr	3.18×10^{-2}	1 hr	5.76×10^{-2}
4 hr	3.39×10^{-2}	4 hr	6.61×10^{-2}
20 hr	3.61×10^{-2}	20 hr	6.20×10^{-2}
24 hr	2.65×10^{-2}	24 hr	6.14×10^{-2}
UV, catalyst & HP		UV & TiO_2	
Time	Conc (M)	Time	Conc (M)
Start	6.33×10^{-2}	Start	7.19×10^{-2}
1 hr	6.13×10^{-2}	1 hr	7.26×10^{-2}
4 hr	6.38×10^{-2}	4 hr	7.31×10^{-2}
20 hr	6.28×10^{-2}	20 hr	6.50×10^{-2}
24 hr	6.25×10^{-2}	24 hr	6.81×10^{-2}

Table 3.5-1: Summary of results of degradation of model whitewater.

3.6 Whitewater

An actual process whitewater was also obtained from Howe Sound Pulp and Paper Mill and was furnished by the UBC group of Prof. J.N. Saddler. It contains carbohydrates, fatty acids and resin acids, lignins, sterols, steryl esters, and triglycerides. The total organic matter concentration is 2-3%.The real

whitewater was treated in the same manner as the model water, as was the data. There was only one run of each treatment done because there was an insufficient amount of the real water to do more than one run.

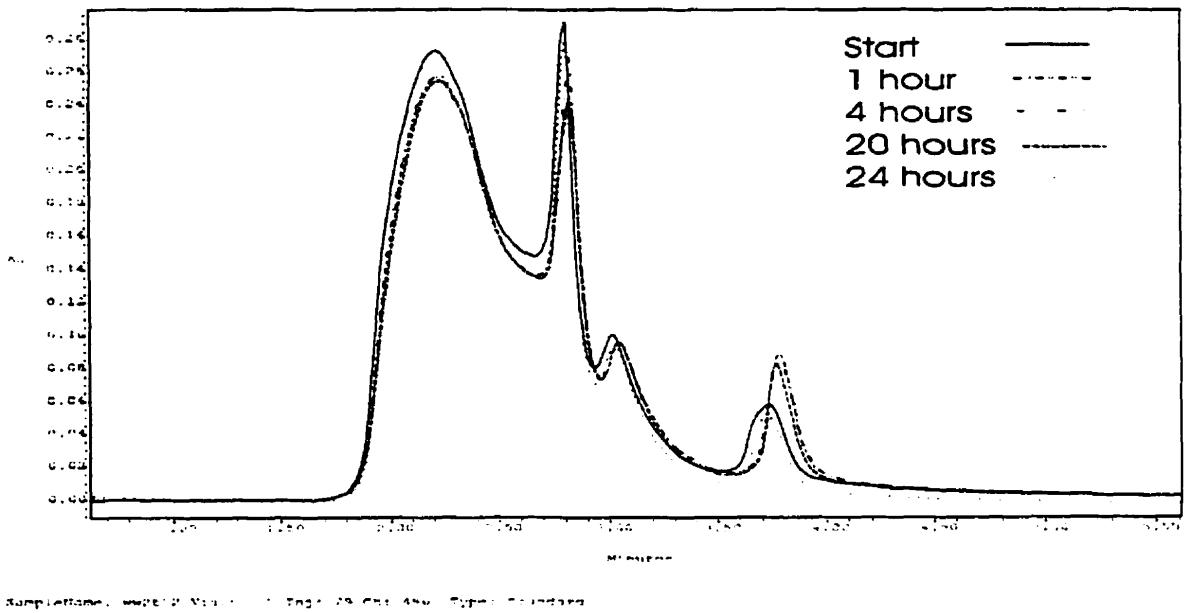

Figure 3.6-1: HPLC chromatogram of aqueous extract of real whitewater treatment with the supported catalyst. This portion contains the lignins. Overlapping peaks were averaged as they are all part of the lignins.

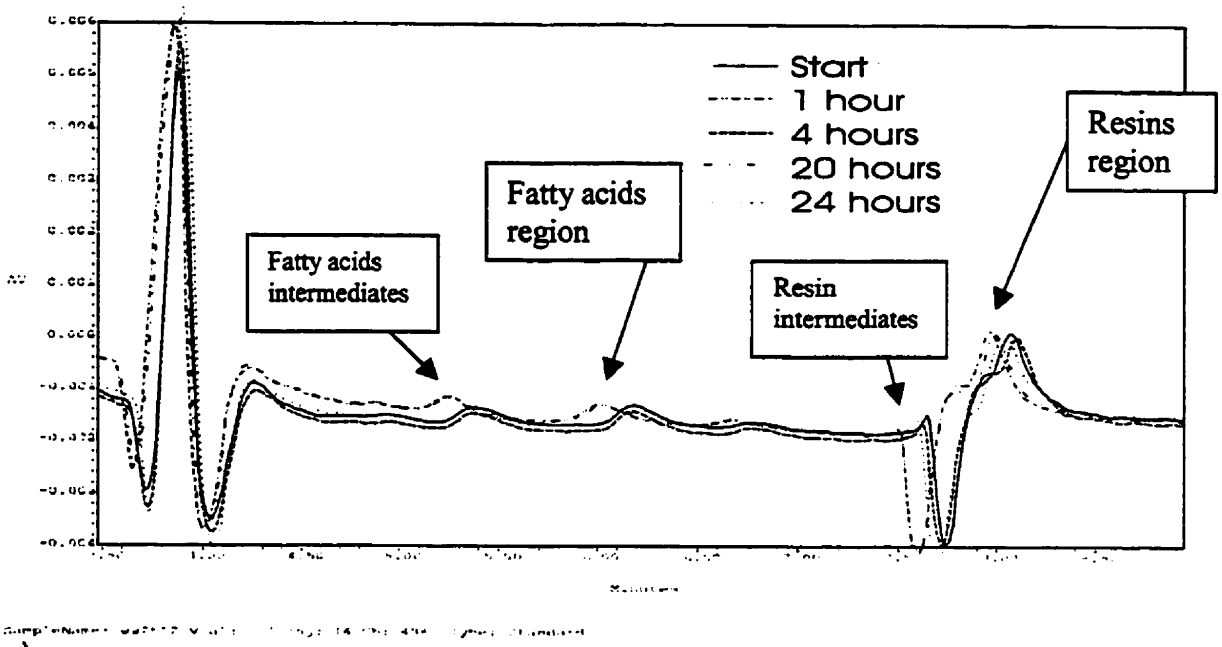

a)

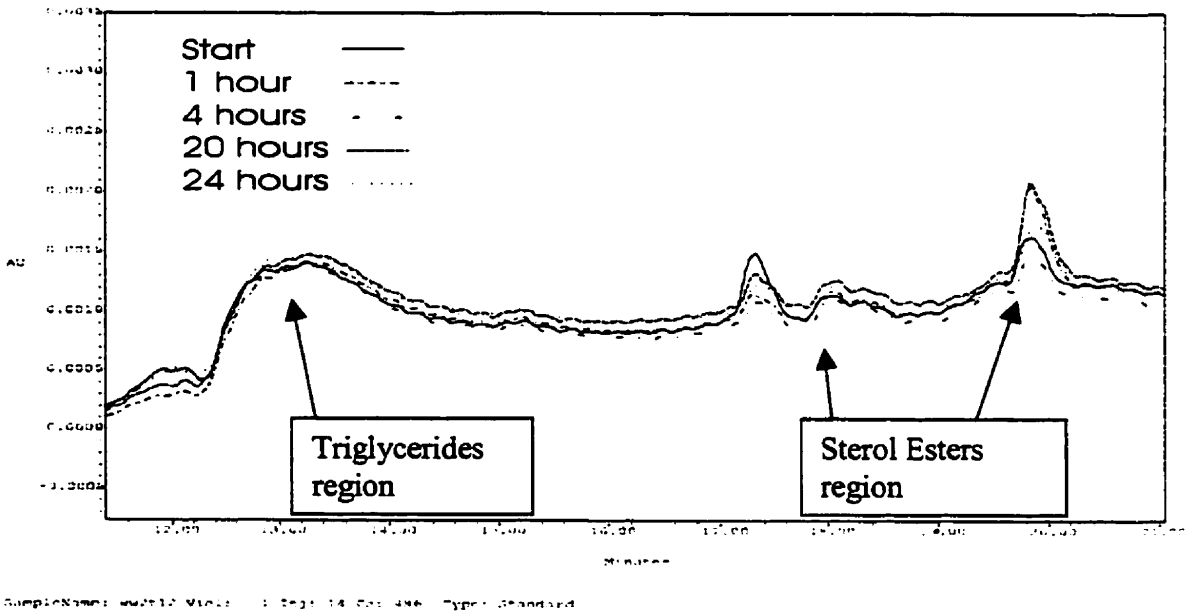

b)

Figure 3.6-2: HPLC chromatogram of the organic extract of the real whitewater treatment with the supported catalyst. This portion contains the fatty acids and resin acids, triglycerides, and sterol esters.

UV-Visible spectrometry of the aqueous extract of the extracted samples showed no discernable bleaching on treatment by direct photolysis and treatment with the supported catalyst, Figure 3.6-3 to 3.6-6.

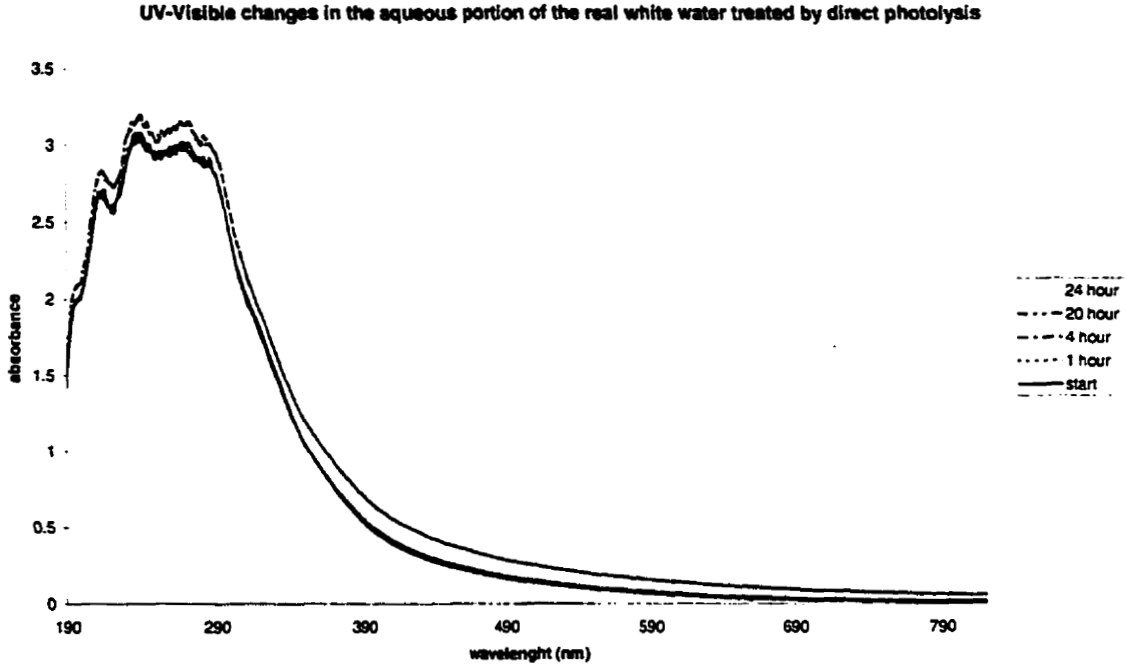

Figure 3.6-3:UV-Visible spectra after direct photolysis on the aqueous portion of real whitewater

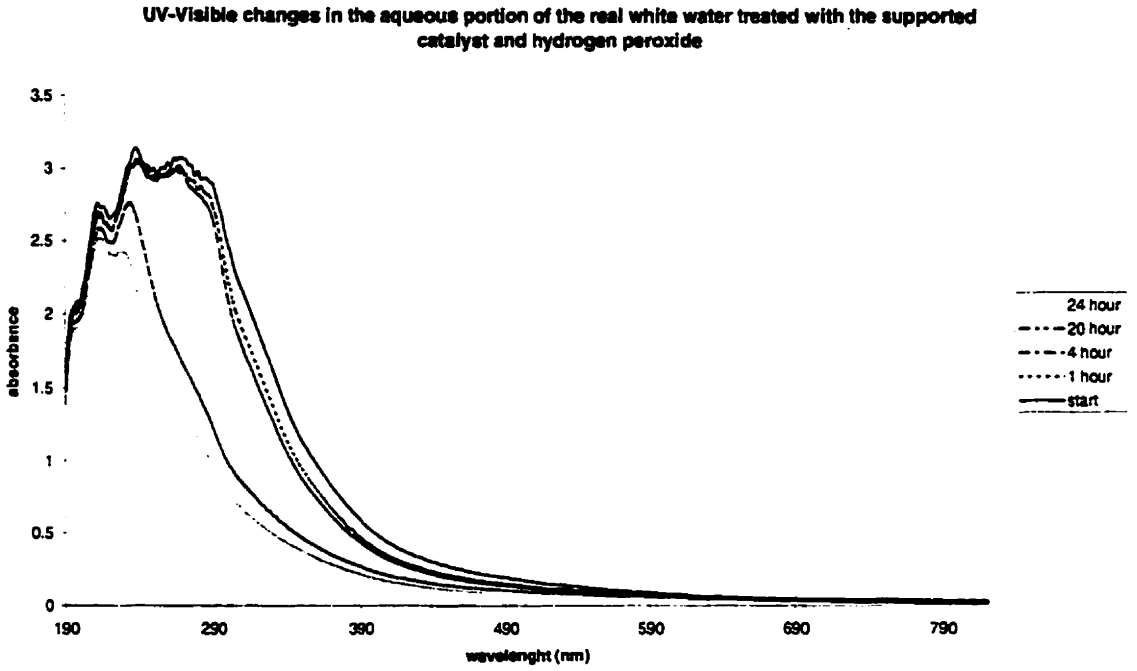

Figure 3.6-4:UV-Visible spectra after treatment of the real whitewater with the supported catalyst

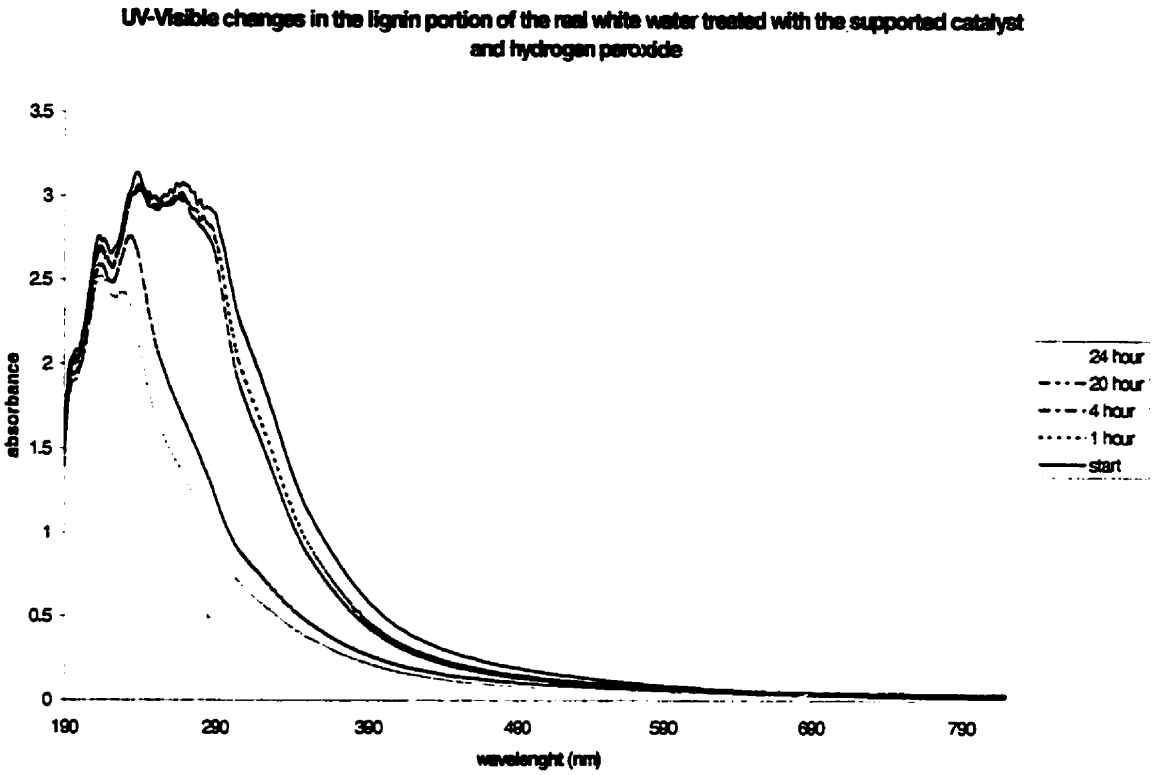

Figure 3.6-5:UV-Visible spectra after treatment of the real whitewater with the supported catalyst and hydrogen peroxide

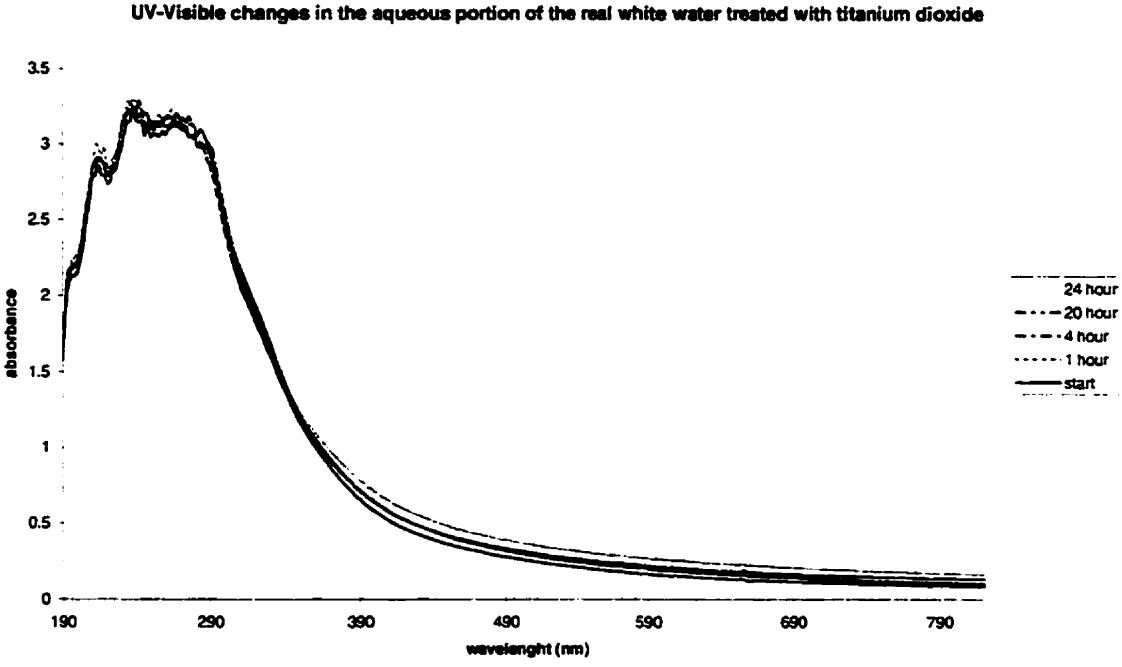

Figure 3.6-6:UV-Visible spectra after treatment of the real whitewater with titania

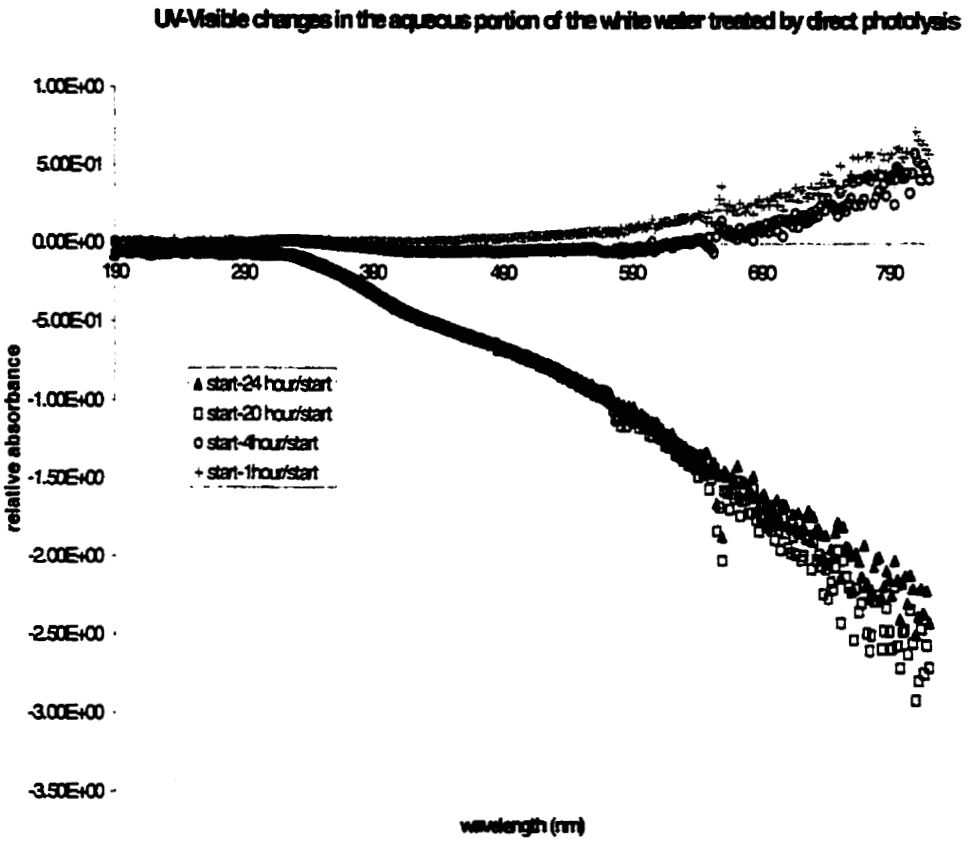

Figure 3.6-7: Differential UV-visible spectra, showing changes occurring during direct photolysis of the aqueous portion of the real water.

However, there was formation of intermediate coloured compounds at 600 nm. Direct photolysis showed only formation of these compounds (Figure 3.6-7).

Treatment with the supported catalyst showed degradation followed by formation of the coloured intermediates, (Figure 3.6-8).

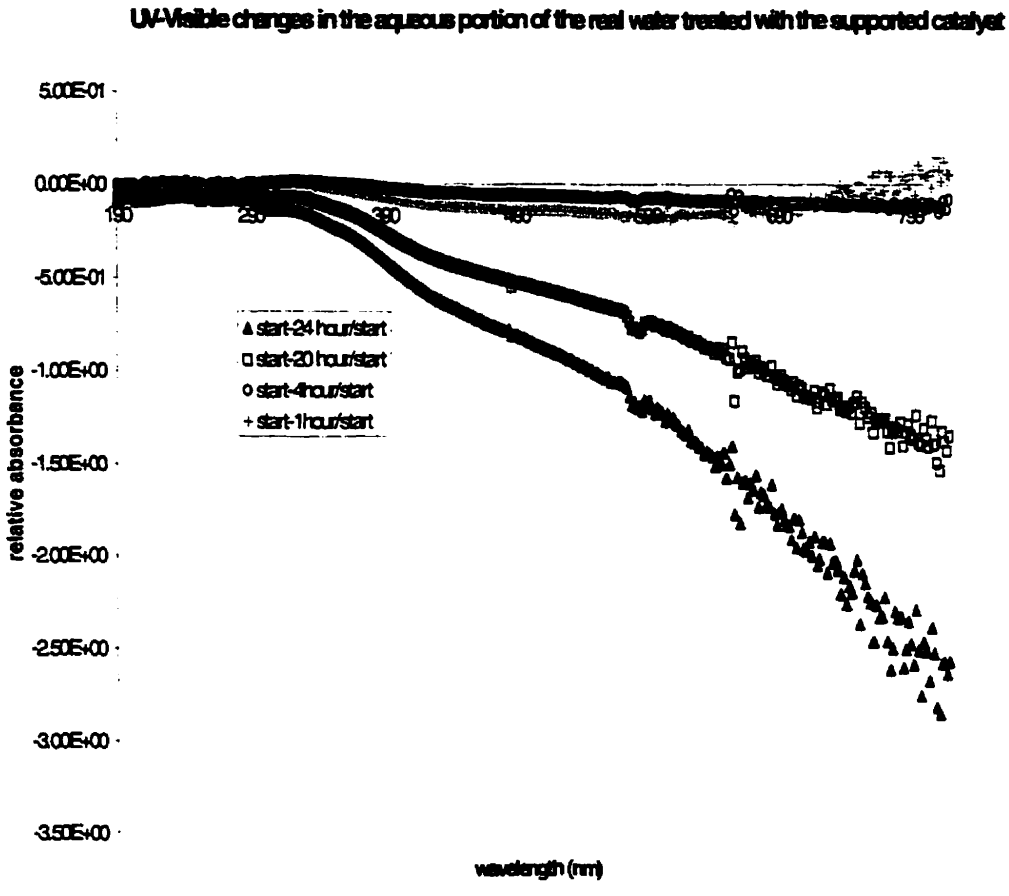

Figure 3.6-8: Differential UV-visible spectra, showing changes occurring during treatment of the aqueous portion of the real water with the supported catalyst.

Treatment with Degussa P25 TiO_2 showed no initial changes; however, some bleaching and formation of coloured intermediates followed by degradation of the coloured compounds is seen, (Figure 3.6-9).

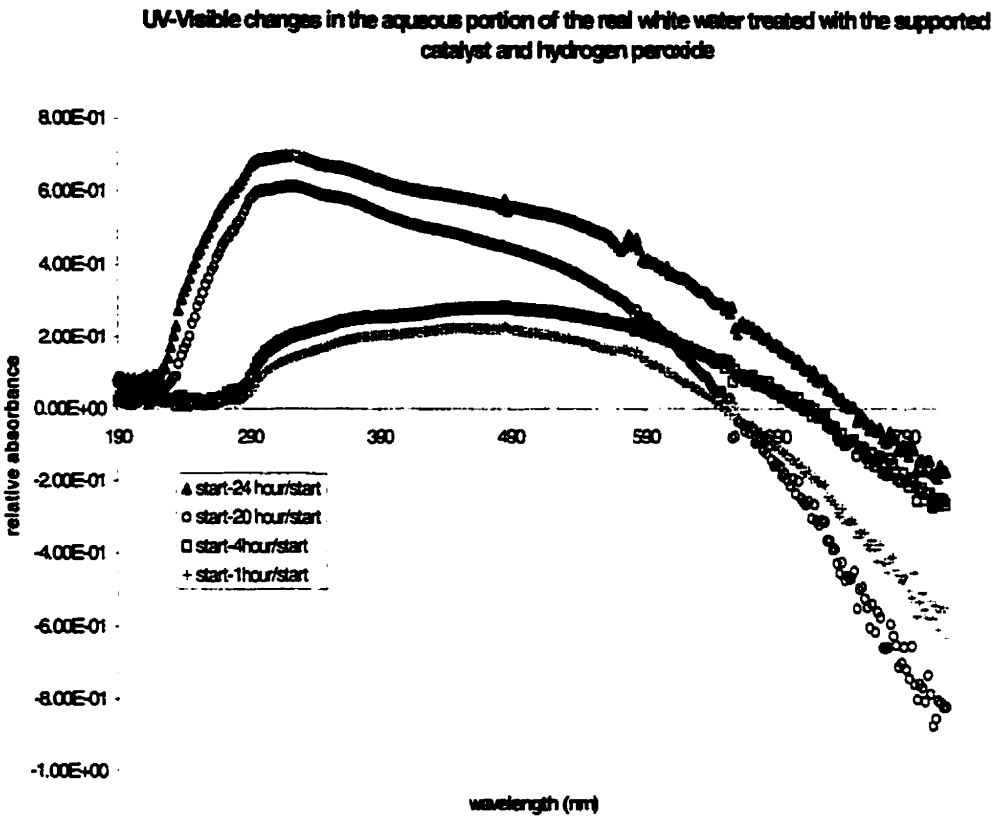

Figure 3.6-9: Differential UV-visible spectra, showing changes occurring during treatment with titanium dioxide.

Treatment with the supported catalyst and hydrogen peroxide showed the largest amount of bleaching and the most formation of coloured intermediates followed by degradation of the intermediates, (Figure 3.6-10).

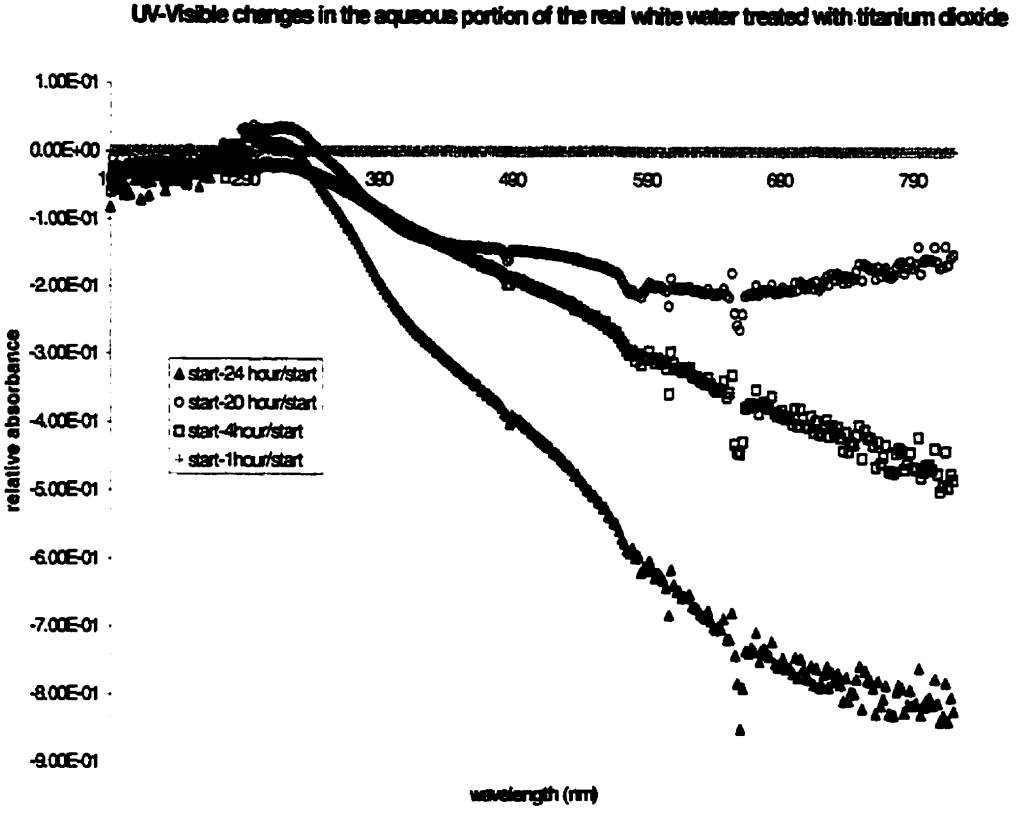

Figure 3.6-10: Differential UV-visible spectra, showing changes occurring during treatment with the supported catalyst and hydrogen peroxide.

Estimated concentration changes in the whitewater can be observed in table 3.6-1 below. The fatty acids in the whitewater were degraded in most cases. With respect to this class of compounds, it appears that the catalyst was the most efficient, resulting in 13.68 % degradation. In addition to this, both UV light and UV light combined with the catalyst and peroxide gave poor reduction, resulting in only 1.86 % and 1.26 % respectively. UV light coupled with titania gave inconclusive results. Resin acids were relatively well degraded in most cases. UV light, UV light with catalyst and UV light with TiO_2 were all comparable giving degradation rates of 27.55 %, 31.66 % and 35.48 % respectively. When the catalyst was coupled with hydrogen peroxide, however, resin acid formation from polymeric

components occurred, resulting in an increase in concentration of 28.92 %. In the case of triglycerides, all reactions resulted in small net degradation of products. UV light and UV light with catalyst and hydrogen peroxide resulted in similar percent overall reductions of 6.72 % and 6.87 % respectively. With UV light and TiO_2, the percent reduction was 2.75 %. With UV light and the catalyst, the overall reduction was only 0.95 %.

Fatty Acids			
UV only		UV & catalyst	
Time	Conc (M)	Time	Conc (M)
Start	3.15×10^{-3}	Start	3.45×10^{-3}
1 hr	3.10×10^{-3}	1 hr	3.34×10^{-3}
4 hr	3.21×10^{-3}	4 hr	3.25×10^{-3}
20 hr	3.20×10^{-3}	20 hr	3.28×10^{-3}
24 hr	3.09×10^{-3}	24 hr	2.98×10^{-3}
UV, catalyst & HP		UV & TiO_2	
Time	Conc (M)	Time	Conc (M)
Start	3.28×10^{-3}	Start	3.14×10^{-3}
1 hr	3.34×10^{-3}	1 hr	3.17×10^{-3}
4 hr	3.31×10^{-3}	4 hr	3.17×10^{-3}
20 hr	3.29×10^{-3}	20 hr	3.35×10^{-3}
24 hr	3.24×10^{-3}	24 hr	3.17×10^{-3}
Resin Acids			
UV only		UV & catalyst	
Time	Conc (M)	Time	Conc (M)
Start	1.78×10^{-3}	Start	1.63×10^{-3}
1 hr	1.68×10^{-3}	1 hr	1.55×10^{-3}
4 hr	1.58×10^{-3}	4 hr	1.42×10^{-3}
20 hr	1.57×10^{-3}	20 hr	1.31×10^{-3}
24 hr	1.29×10^{-3}	24 hr	1.12×10^{-3}

UV, catalyst & HP		UV & TiO_2	
Time	Conc (M)	Time	Conc (M)
Start	1.11×10^{-3}	Start	1.42×10^{-3}
1 hr	8.15×10^{-4}	1 hr	1.33×10^{-3}
4 hr	1.19×10^{-3}	4 hr	1.08×10^{-3}
20 hr	1.56×10^{-3}	20 hr	1.08×10^{-3}
24 hr	1.44×10^{-3}	24 hr	9.17×10^{-4}
Triglycerides			
UV only		UV & catalyst	
Time	Conc (M)	Time	Conc (M)
Start	7.47×10^{-2}	Start	6.14×10^{-2}
1 hr	6.71×10^{-2}	1 hr	5.81×10^{-2}
4 hr	8.37×10^{-2}	4 hr	6.49×10^{-2}
20 hr	6.82×10^{-2}	20 hr	6.22×10^{-2}
24 hr	6.97×10^{-2}	24 hr	6.08×10^{-2}
UV, catalyst & HP		UV & TiO_2	
Time	Conc (M)	Time	Conc (M)
Start	6.02×10^{-2}	Start	6.00×10^{-2}
1 hr	5.93×10^{-2}	1 hr	5.90×10^{-2}
4 hr	4.24×10^{-2}	4 hr	5.88×10^{-2}
20 hr	6.28×10^{-2}	20 hr	5.82×10^{-2}
24 hr	5.61×10^{-2}	24 hr	5.84×10^{-2}

Table 3.6-1: Concentrations of compounds in model water throughout the 24 hour irradiation period

3.7 Comparison of Model Whitewater with Real Whitewater.

Generally speaking, the model whitewater and real whitewater behaved comparably, but also in a slightly different fashion. In both the model whitewater and the real whitewater, the catalyst with UV light resulted in the greatest levels of overall degradation, 3.42 % and 13.68 % respectively. In the model whitewater,

however, use of hydrogen peroxide with the catalyst resulted in formation of more fatty acids from polymeric constituents. In the model whitewater and real whitewater, it appears that TiO_2 in the presence of light gave relatively good results of 24.87 % and 35.48 % degradation respectively. In the case of the real whitewater, coupling the catalyst with hydrogen peroxide resulted in large net formation of resin acids from polymers, 28.92%, while in the model whitewater, this resulted in the largest apparent degradation, a percent reduction of 31.18 %. In the triglycerides, we can suggest that irradiation with UV light, in both the model and real whitewaters was quite effective, resulting in percent degradations of 15.10% and 6.72 % respectively. In the real whitewater, addition of hydrogen peroxide to the whitewater resulted in slightly increased degradation of 6.87 %. UV light with catalyst in the model whitewater resulted in the second best percent reduction of 14.14 %.

Overall, we can make some general conclusions. First, UV light with the catalyst is generally a good method of photocatalysis simply because in both the model water and whitewater, increase of the target compounds is not seen. In the model whitewater, we can suggest that the overall, best treatment appears to be TiO_2 with UV light. However, we can suggest that since irradiation of the model whitewater occurred only for 24 hours, the hydrogen peroxide with the catalyst may be better because although intermediate formation has, at this point, occurred, further irradiation may result in increased degradation. In the case of the real whitewater, we can suggest that UV light with the catalyst is the best apparent treatment, giving degradation in high or comparable levels in all cases. Again,

however, irradiation only occurred for a period of 24 hours, and thus, we can suggest that if irradiation was allowed to occur for longer periods of time, the product formation observed with the catalyst and hydrogen peroxide may degrade, resulting in this method being the best technique.

4 Discussion

4.1 Hydrogen Peroxide Coupled with Catalytic Degradation

The variation of "overall" degradation as measured by decrease of HPLC peak area or UV absorbance in a region attributed from the model studies to one class of constituents shows that a complexity in this study is the sequence of:

Primary constituent → intermediate → CO_2, etc.

The polymeric primary constituents can produce oxidation intermediates that correspond to the smaller molecular constituents and make net degradation small. When this is fully taken into account, the best oxidation system is probably the supported catalyst promoted by H_2O_2.

We can suggest, for numerous reasons, that peroxide coupled with the supported catalyst is the best oxidation treatment. First, it is known that H_2O_2 is an initiator in organic oxidation reactions, thus greatly increasing the rate of degradation of individual classes of compounds.[1],[2] In addition to this, we have observed that when degradation is occurring on model compounds, this treatment appears to be the most beneficial treatment. The supported catalyst is beneficial because it acts as an adsorbent preconcentrator both a source of electrons and a source of ·OH. When peroxide is added to the reaction mixture, it results in a substantial increase in the amounts of, ·OH, thus greatly improving the oxidation efficiency of the system.

One problem associated with photocatalysis in any case is the decreased efficiency resulting from recombination of the hydroxyl radicals with free electrons.

Increasing recombination results in decreased efficiency. With an excess of ·OH, it implies that the opportunity of recombination of these radicals with electrons is now decreased, allowing an excess of ·OH to remain in solution. In addition to this, the hydroxyl radical is a powerful oxidant, which can react with many different substrates. Hydrogen atom extraction by the radical results in the rapid degradation of saturated organic compounds coupled with hydroxide ion formation. Unsaturated organic compounds pose only slightly more of a challenge, although reaction of these compounds generally occurs via ·OH addition to the double bond may result in epoxide formation.[3]

4.2 Development of a New Monitoring Method

We have assigned chromatogram areas to retention time regions for each of the model compounds and created calibration curves. Second, we have considered aqueous solutions and organic solvent extracts. These seem to provide sensible descriptions of the reaction sequences for the model and "real" whitewater samples. Even if our analysis scheme is not exact with respect to structural chemistry, the combination of HPLC, extractions and UV-visible spectrometry is promising as a method for monitoring whitewaters. The method in each application, unique to each plant, should be calibrated against the old "complex" analysis in order to thoroughly link the results of the two separate methods.

Initial analysis of whitewaters using the "complex" method will allow complete information to be obtained about the composition of the whitewater in question. Following this, analysis of these same waters with the simpler technique will allow for direct correlation of results. This initial correlation will allow for semi-quantitative analysis to occur. Furthermore, combination of these analyses will allow for general monitoring with a simple method to ensure that environmental standards are met. Monthly and/or annual repetition of the "complex" method will allow for confirmation of correlation and quantitative analysis to occur.

The new method is beneficial because of the decreased time requirements in order to achieve full information about the composition of the system. Although no specific information is given about compound structure and quantity of each individual compound, regulations tend to deal with collections of compounds nonetheless. As such, this method is effective in reducing time requirements and cost associated with the existing method of quantitation in whitewater systems.

Since generally, chromatography appears to be the method of choice, as shown in Figure 1.5-1, this method simply provides a means of observing content without isolation of each compound in question. This is critical in accelerating the analysis of whitewaters to allow for rapid correction of problems as opposed to present methods, which can result in problems remaining untreated for days or longer. Especially, in the case of the more toxic compounds such as resin acids, this will, in the long run, prove to be beneficial.

Environmental guidelines are set in order to ensure that toxicity of compounds does not become lethal to fish and other aquatic life. This technique

provides a routine method for routine analysis of whitewaters and their content. As such, we can suggest that this method is widely applicable, fast and reliable. It is also semi-quantitative, which will permit quality control and consequent compliance with water safety standards.

4.3 General Conclusions

We can suggest that overall the catalyst coupled with peroxide is an efficient oxidant and thus, an effective means of breaking down organic contaminants. Observations have suggested that with model whitewater, as in the case of real whitewater formation of some of the compounds can occur from larger, polymeric materials. We have noted previously, that UV light with the catalyst appears to be the most efficient method of degradation simply because toxic product formation does not appear to occur. In the model white water, TiO_2 with UV light appears to be an effective method of treatment. As previously suggested, however, we also suggest that combination of peroxide with catalyst and light will result in the best overall degradation of products if the reaction is given sufficient time to go to completion.

References

1. Sustainable Forest Management. UBC reports #2 and #3.

2. Vaisman, E, M.Sc. Thesis University of Calgary, **1999**, 78-80.

3. March, J. "Advanced Organic Chemistry". **1992,** 4th ed., 823.

Appendix 1

Sample Calculation for Concentration of Compounds

Done with vinyl acetic acid sample taken at t = 24 hours for treatment with the catalyst

Peak area = 30776 area units

Calibration curve equation: $y = (5.02788 \times 10^{6})x - 1.19091 \times 10^{4}$

Concentration of vinyl acetic acid at t = 24 hours is 8.50×10^{-3} M

The samples of model water and real whitewater were calculated with the same method

Sample Calculation for the Relative Percent Reduction of the Compound

Done with vinyl acetic acid treatment with the catalyst

Concentration at start = 1.15×10^{-2} M

Concentration after treatment = 8.50×10^{-3} M

Relative percent reduction = $\frac{1.15 \times 10^{-2} - 8.50 \times 10^{-3}}{1.15 \times 10^{-2}} \times 100 = 26.09\ \%$